공학석사 학위논문

Response Pattern Analysis of Human Olfactory Receptors to Indole

인돌에 대한 인간 후각 수용체의 반응 패턴 분석

2020년 8월

서울대학교 대학원

공과대학 협동과정 바이오엔지니어링 전공

강 은 진

Abstract

Response Pattern Analysis of Human Olfactory Receptors to Indole

Eunjin Kang

Interdisciplinary Program in Bioengineering

The Graduate School

Seoul National University

Human olfaction starts with selective binding of odorants to olfactory receptors (ORs) in nasal mucus. The combinatorial patterns of ORs stimulated by odorants are believed to decide the odor perception. The affinity between an OR and an odorous molecule is defined by their various molecular properties and other chemical aspects in a complicated manner. Thus, it is genuinely difficult to define which ORs an odorant will bind, and what description of smell the molecule will drive simply by considering their properties. In this study, odors of selected odorants were analyzed with an approach to the overall combinatorial patterns of 388 ORs instead of the individual OR responses. Visualization methods that represent an odor in terms of sensitivities and response levels of 388 human ORs to the odorous molecule were suggested and used to analyze and compare OR response patterns.

Indole, methyl dihydrojasmonate and naphthalene were selected to compare OR response patterns. The perceived smell of indole differs by its concentrations. Indole at low concentration smells like jasmine, similar to the smell of methyl dihydrojasmonate. In contrast, the smell of indole at high concentration is perceived like mothball as naphthalene. Indole and methyl dihydrojasmonate are structurally distant, but indole and naphthalene are heterocyclic analogues that contain benzene ring(s).

The response levels of ORs to each odorant were measured by a heterologous system established in Hana3A cells, which stably express accessory proteins that support robust cell surface expression of membrane proteins. The cAMP level increased by OR activation was measured using luciferase assay. The number of responsive ORs and response intensities to indole were positively correlated with indole concentration. Comparing the response patterns of three different odorants, ORs that recognize one or more than one of the odorants were found. The response intensities of responsive ORs showed greater similarities when the molecular structures of odorants were closer. There was a positive correlation between the perceived strength of the smell and the number of responsive ORs. Considering the protein similarity among same OR subfamily members, the OR response patterns were also analyzed at the subfamily level. Patterning of OR responses at the subfamily level was sufficient to distinguish and compare the OR response patterns of different odors. The number of common responsive subfamilies between odorants were much greater than that of the common responsive OR proteins. Increase of indole concentration led to higher similarity of response pattern with the pattern of naphthalene than that with methyl dihydrojasmonate. Even though there were

some matching ORs and subfamilies between response patterns of similar odors, the patterns were very unique and distinguishable. These results show that the response of ORs to odorants is much more complicated and specific than what we actually interpret and perceive. This supports higher sensitivity and accuracy of OR based electrical devices to detect target chemicals than animal-based chemical detection. Because the visualization process excludes many natural mechanisms that occur in nasal mucus and neuronal systems, this encoding method for odors will allow objective recording of smell with least genetic and individual variations and contribute to standardization of olfaction and further understanding of the sense of smell.

Keywords: olfaction, human olfaction, odor perception, olfactory receptor, indole, olfaction standardization, odor visualization, odor codification, luciferase assay, heterologous cell system

Student number: 2018-21289

Table of Contents

List of Tables and Figures

1. Introduction

1.1. Human olfaction

1.1.1. Olfactory mechanism

Olfaction is an essential and complex system to recognize beneficial and harmful chemicals in the environment. That the largest superfamily of genes, about 400 of 20,000 human genes, is devoted to olfactory receptors (ORs) supports the significance of the olfactory system [1, 2]. Olfaction starts with stimulation of ORs in mucus in the nasal cavity followed by signal transduction towards the olfactory bulb (OB) and the olfactory cortex [3, 4]. Each receptor has different affinity to an odorous molecule. The stimulation level of each receptor and the combinatorial pattern of receptors are delivered to decide the odor description of the given odorant [5, 6].

1.1.2. Olfactory receptors and nomenclature

ORs are seven-transmembrane domain proteins, and the OR gene superfamily contains 388 functional genes and 456 pseudogenes [5, 7, 8, 9]. The most officially used nomenclature system of the ORs is called hORDE and based on the protein sequence similarity and a divergence evolutionary model [9]. The hORDE system consists of the superfamily name 'OR' followed by the family numbers, subfamily letters, and individual numbers within the subfamily (Fig. 1, Table 1). The functional OR proteins are arranged into 17 families that share >40% protein identity, and each family is divided into multiple subfamilies that have >60% protein identity. There was evidence of an aspect that ORs with related sequences are more likely to recognize structurally similar ligands [2]. However, the relation between OR protein sequences and their binding site is still unknown.

Numerous efforts to predict odors by demonstrating affinities between ORs and odorants using their structures have been made [10, 11, 12, 13]. There were a few relations between chemical properties of odorants and their affinities to ORs [2], and some ORs were deorphanized [11, 13, 14, 15,16]. However, there still are lots of exceptions, and the chemical properties are insufficient to understand and predict the smell of odorants [17, 18].

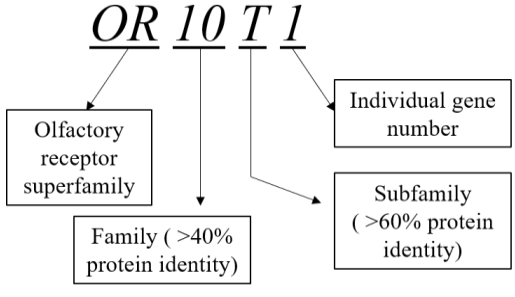

Figure 1. hORDE: Human Olfactory Receptor Nomenclature

Table 1. Summary of OR Gene Families

Family	Subfamilies (No. of Functional Genes in Each Subfamily)	No. of Subfamilies	No. of Functional Genes
1	A(2), B(1), C(1), D(3), E(2), F(2), G(1), I(1), J(3), K(1), l(5), M(1), N(2), Q(1), S(2)	15	28
2	A(8), B(4), C(2), D(2), F(2), G(3), H(2), J(2), K(1), L(5), M(5), S(1), T(16), V(2), W(3), Y(1), Z(1), AE(1), AG(2), AJ(1), AK(1), AP(1), AT(1)	23	67
3	A(4)	1	4
4	A(4), B(1), C(10), D(7), E(1), F(7), K(7), L(1), M(2), N(3), P(1), Q(1), S(2), X(2)	14	49
5	A(2), B(5), C(1), D(4), F(1), H(5), I(1), J(1), K(4), L(2), M(6), P(2), R(1), T(3), V(1), W(1), AC(1), AK(1), AN(1), AP(1), AR(1), AS(1), AU(1)	23	47
6	A(1), B(3), C(11), F(1), J(1), K(3), M(1), N(2), P(1),Q(1), S(1), T(1), V(1), X(1), Y(1)	15	30
7	A(3), C(2), D(2), E(1), G(3)	5	11
8	A(1), B(5), D(3), G(2), H(3), I(1), J(2), K(3), S(1), U(3)	10	24
9	A(2), G(3), I(1), K(1), Q(2)	5	9
10	A(6), C(1), D(1), G(7), H(5), J(3), K(2), P(1), Q(1), R(1), S(1), T(1), V(1), W(1), X(1), Z(1), AD(1), AG(1)	18	36
11	A(1), G(1), H(5), L(1)	4	8
12	D(2)	1	2
13	A(1), C(6), D(1), F(1), G(1), H(1), J(1)	7	12
14	A(2), C(1), I(1), J(1), K(1)	5	6
51	A(3), B(4), D(1), E(2), F(2), G(2), I(2), J(1), L(1), M(1), Q(1), S(1), T(1), V(1)	14	23
52	A(3), B(3), D(1), E(5), H(1), I(2), J(1), K(2), L(1), M(1), N(4), R(1), W(1)	13	26
56	A(4), B(2)	2	6
		175	**388**

1.2. Visualization of OR response patterns

There are difficulties in prediction of smell only by interactions between ORs and odorants using their structures and chemical properties. As a dramatic number of cases of combinatorial response patterns of 388 ORs are possible, approaches to smell with the overall OR response patterns will give further insights to understanding of olfaction. It will also bridge the uncertainty of structural approaches to odors and odor perception. Furthermore, codification of the response levels of 388 ORs will ease analysis and comparison of smell at the receptor level (Fig. 2).

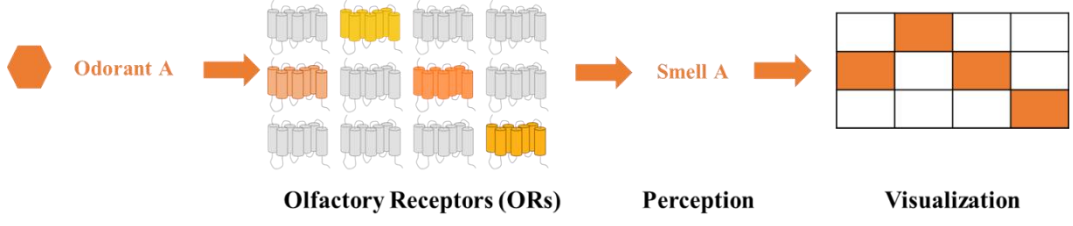

Figure 2. Combinatorial Response and Visualization of Olfactory Receptors

1.3.Luciferase assay

In an intrinsic human olfactory sensory neuron, activation of an OR by odorous molecule binding initiates GPCR signal cascade that activates the enzyme, adenylyl cyclase type 3(ACIII) (Fig. 3a) [19]. AC family increases the concentration of cyclic adenosine monophosphate (cAMP). cAMP opens cyclic nucleotide-gated ion channels (CNG) that drives calcium (Ca^{2+}) and sodium (Na^{+}) ion influx and increases their concentrations inside the cell. The increased concentration of Ca^{2+} inside the cell activates the $Ca2^{+}$-dependent chloride (cl^{-}) that transport intracellular Cl^{-} to outside of the cell. Augmented depolarization stimulates action potentials that initiate neuronal signal transduction.

The heterologous system in OR expressing Hana3A cells uses the increase of cAMP by OR activation (Fig. 3b) [20]. Increase of cAMP level activates cAMP dependent protein kinase A (PKA) which phosphorylates a cellular transcription factor, CRE binding protein (CREB). Phosphorylated CREB is translocated into the nucleus, and its binding to CRE promoter initiates transcription of the downstream luciferase gene. Translated luciferase proteins catalyze luciferin and produce bioluminescence whose measurement represents the activation level of OR proteins.

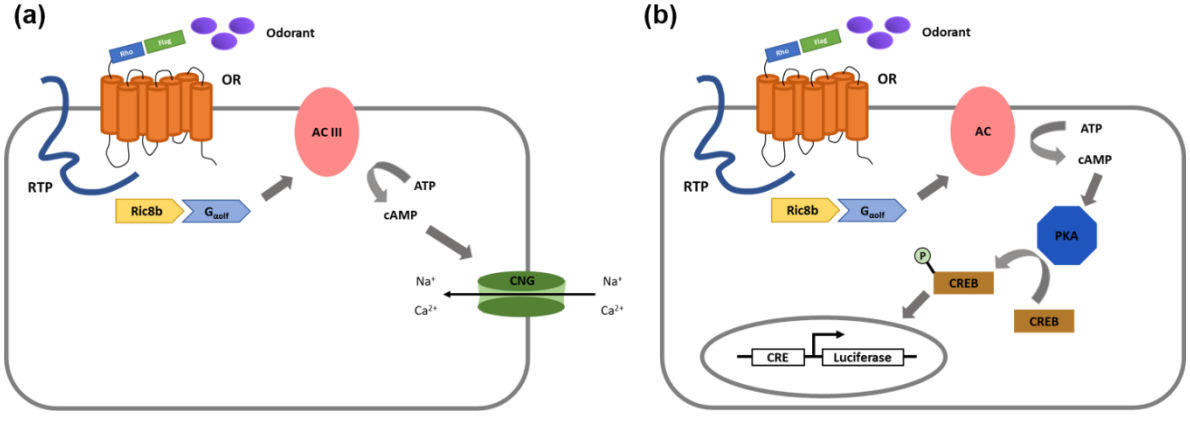

Figure 3. Luciferase Assay Mechanism for OR Response Measurement

(a) cAMP-based signal cascade activated by odorant binding to OR in intrinsic OSN. (b) Luciferase gene expression mechanism by odorant binding to heterologously expressed ORs on Hana3A. RTP: receptor transporting protein, AC (III): adenylyl cyclase (type III), $G_{\alpha olf}$: guanine nucleotide-binding protein G(olf) subunit alpha, CNG: cyclic nucleotide-gated ion channel, PKA: protein kinase A, CRE: cAMP response element, CREB: cAMP response-element binding protein

1.4. Indole

Indole is an aromatic heterocyclic organic compound consisting of a benzene ring and a pyrrole ring. The smell description of indole differs by its concentration. Indole at high concentration is perceived as feces and mothball. In contrast, the smell of indole at low concentration is floral and similar to jasmine scent. Indeed, indole is produced by several flowers including jasmine and orange blossom. Nevertheless, indole is one of the major components of bad odors such as feces, wastewater, bacterial fermentation and breath odor [21, 22, 23, 24].

2. Methods and materials

2.1.Hana3A cell culture

Hana3A is a HEK293 derived cell line that stably expresses multiple accessory proteins including RTP1L, RTP2, REPP1 and $G_{\alpha olf}$ [20]. RTP family members translocate OR proteins to the plasma membrane and induce their functional expression [25]. REEP1 also enhances expression and functionality of ORs but has weaker effects compared to RTP proteins. Gαolf is an olfactory specific G-protein required for signal transduction [26].

Hana3A cells were grown in M10 (10% (vol/vol) FBS supplemented MEM (Gibco, USA)) for transfection and luciferase assay. Hana3A cells were maintained in M10 supplemented with final concentration of 100 μg/ml penicillin-streptomycin (Sigma Aldrich, USA), 1.25 μg/ml amphotericin (Sigma Aldrich, USA) and 1 μg/ml puromycin (Sigma Aldrich, USA). Cells were cultured in a 37°C incubator with 5% CO_2.

Hana3A cells were frozen to make stocks before their 5th passage. For experiment, cells under 10th passage after being thawed were used. Cells had to be trypsinized every other day, and a quarter of the 100% confluent cells were maintained.

2.2.OR gene cloning

OR genes were engineered to express FLAG-tag and Rho-tag. FLAG-tag is to confirm OR expression on the cell surface, and Rho-tag is to support GPCR expression on the plasmid membrane [16, 27]. The recombinant OR DNA was amplified by PCR and inserted to the pcDNA3.0 vector (Fig. 4). Insertion of the target DNA in the vector was confirmed by Sanger DNA sequencing. Vectors with the target DNA were amplified and purified using Fastlon Plus Plasmid Midi Kit (RBC, Taiwan).

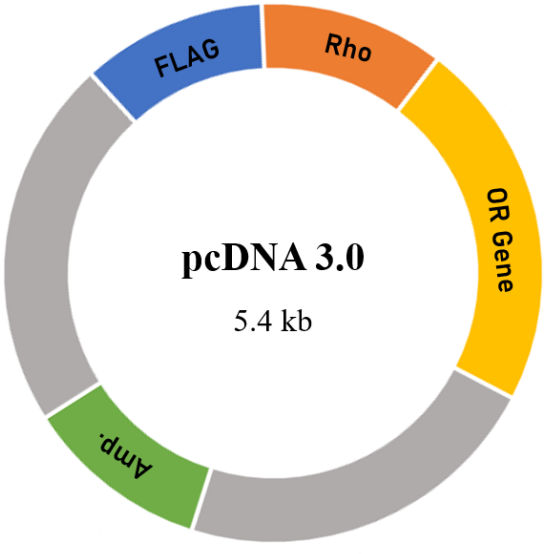

Figure 4. OR Gene Inserted pcDNA3.0 Construct

FLAG: FLAG-tag (DYKDDDDK), Rho: rhodopsin-tag, Amp.: ampicillin resistance gene.

2.3. Heterologous cell surface expression of ORs and confirmation

2.3.1. Transfection

OR genes were introduced into Hana3A cells by transfection using Lipofectamine 3000 (Invitrogen, USA). Along with OR genes, luciferase genes and accessory proteins that enhance the cell-surface expression of ORs were co-transfected (Table 2) [20, 28, 29, 30]. M10 medium without antibiotics was used to minimize toxicity of antibiotics to cells with permeabilized surface by Lipofectamine 3000 reagents. Transfection reagents were applied when the cell confluency was ~50%. After application of the transfection reagents, cells were incubated at 37℃ with 5% CO_2 at least for 20 hours.

Table 2. Transfection Chart

Plasmid DNA	Amount (ng/well)
OR	40
pCRE-Luc	40
pSV40-*Renilla*	10
RTP1S	10
M3-R	5

2.3.2. Western blot

Heterologous expression of OR proteins on the Hana3A cell surface was confirmed by western blot analysis. Hana3A cells were cultures in three T75 (15ml) flasks and transfected with the mock vector and OR1A1 for 20 hours. FLAG-tag was detected by DYKDDDDK tag mouse mAb (Cell Signaling, USA) and β-actin was detected by β-actin mouse monoclonal IgG (Santa Cruz, USA). the secondary antibody was Goat anti-mouse IgG-HRP (AbFrontier, Korea) and used to detect both FLAG-tag and β-actin antibodies. The HRP on the secondary antibody was detected by TOPview ECL Pico Plus Western Substrate (Enzynomics, Korea), and the presence of the target proteins were confirmed.

2.4.OR stimulation

Cell media was changed to CD293 (Gibco, USA). Powders of indole (Sigma Aldrich, USA), methyl dihydrojasmonate (Sigma Aldrich, USA), and naphthalene (Sigma Aldrich, USA) were diluted in DMSO (Sigma Aldrich, USA) to make 1 M stocks. 1M odorants were serially diluted with DMSO and CD293 to make the target final concentration. The final concentration of DMSO was below 1% (vol/vol) in CD293 due to its toxicity to cells [31]. For example, no more than 1 μl of odorant in DMSO was added to 100 μl of the total volume with CD293 for 96-well plate.

The negative control (no-odorant) was OR transfected cells stimulated by DMSO only (0 M of an odorant). After the application of odorants, cells were incubated at 37℃ with 5% CO_2 for 4 hours.

2.5.Cytotoxicity of odorants

Cytotoxicity of each odorant to transfected Hana3A cells were tested using CCK-8 kit (Dojindo, Japan). Cell viability was measured by proliferation ability of cells. Viable cells can catalyze WST-8 and turn the color of WST-8 from yellow to orange-red. The level of color change was measured by Spark 10M multimode microplate reader (Tecan, Switzerland).

Cells were transfected with mock vectors for 20 hours and stimulated with 0 M, 10 nM, 100 nM 1 μM, 10 μM, 100 μM, 1 mM, 10 mM of indole, methyl dihydrojasmonate and naphthalene respectively. Cell viability after 4 hours of stimulation was measured.

2.6. Measurement of OR responses

2.6.1. Selection of responsive ORs

The level of OR responses to odorants were measured by luciferase assay (Fig. 3b) using Dual-glo Luciferase assay system (Promega, USA). CRE-mediated firefly luciferase activity represents the OR activation level, and the bioluminescence production was measured by Spark 10M multimode microplate reader. In addition, constitutively active SV40 promoter-mediated Renilla luciferase activity was used to measure the transfection efficiency and the cell number. The firefly luciferase activity measurements were normalized with Renilla luciferase measurements as below.

$$\mathrm{N} = \mathrm{Luc}/\mathrm{Ren}$$

$$\frac{\Delta N}{N} = \frac{N(odorant) - N(no - odorant)}{N(no - odorant)}$$

To minimize the variation from the transiently transfected cell-based assay, data of six replicates, whose coefficient of variation (CV) was below 0.15, were used. t-test was conducted for the data of an OR in presence and absence of an odorant. ORs with $p<0.05$ were considered responsive, except for indole. For indole, there were ORs that had high ΔN/N values but had p-values higher than 0.05. Among those ORs, those with higher ΔN/N than the smallest ΔN/N of statistically significant responsive OR (OR10V1; 0.103, Table 3) were additionally selected not to miss responsive ORs due to the variations caused by the cell-based assay.

2.6.2. Dose-response test

Dose-response tests were conducted for indole only. First, positively responding ORs to indole were stimulated with 0 M, 1 μM, 10 μM, and 100 μM of indole and their response levels to each concentration was measured. All were tested with three replicates. According to the results, responsive ORs were grouped into 3: ORs that responded to 1 μM were grouped in the high sensitivity group, ORs that did not respond to 1 μM but responded to 10 μM and 100 μM were grouped into the medium sensitivity group, and ORs that only reacted to 100 μM were grouped into the low sensitivity group.

Dose-response tests were conducted according to the designated groups. The high sensitivity group was tested with 0 M, 1 nM, 10 nM, 100 nM, 1 μM, 10 μM, 100 μM, and 1mM. The medium sensitivity group was tested with 0 M, 1 μM, 3 μM, 10 μM, 30 μM, 100 μM, 300 μM, and 1mM. The low sensitivity group was excluded from the dose-response test. All were tested with 6 replicates.

Dose-dependent sigmoidal curves of responsive ORs were drawn, and EC_{50} were obtained using GraphPad Prism 7 software program. For the dose-response curves, the logarithm of odorant concentrations and firefly / Renilla ratios (Luc/REN) were used. The ratios were normalized such that the lowest value was set to 0% and the highest to 100%.

2.7. Visualization of OR response patterns

Patterns of OR responses were visualized using heatmaps. Three types of OR arrangement for visualization was used. The first type was arrangement of OR genes on a square 20x20 matrix in the order of hORDE nomenclature (Fig. 5a). For the second arrangement according to the OR family (Fig. 5b), the family numbers were aligned along the vertical axis, and the members of each family were enumerated according to the nomenclature. The third type was to analyze the response of OR subfamilies. Each cell determines the subfamily name, and the responding OR fraction per each family was used (Fig. 5c)

Heatmaps were drawn using GraphPad Prism 7 software program. For the representative patterns of an odorant, the logarithm of the sensitivity, $\log(1/EC_{50})$, was used. Values were ranged from 4 to 10. The response patterns at certain concentrations display $\Delta N/N$ values ranging from 0 to 1. For the subfamily responses, the fraction of positively responding ORs in a subfamily (No. responsive ORs)/ (No. member of ORs in the subfamily), ranging from 0 to 1, was used.

(a)

	A	B	C	D	E	F	G	H	I	J	K	L	M	N	O	P	Q	R	S	T
1	OR1A1	OR1A2	OR1B1	OR1C1	OR1D2	OR1D4	OR1D5	OR1E1	OR1E2	OR1F1	OR1F12	OR1G1	OR1I1	OR1J1	OR1J2	OR1J4	OR1K1	OR1L1	OR1L3	OR1L4
2	OR1L6	OR1L8	OR1M1	OR1N1	OR1N2	OR1Q1	OR1S1	OR1S2	OR2A1	OR2A2	OR2A4	OR2A5	OR2A7	OR2A12	OR2A14	OR2A25	OR2B2	OR2B3	OR2B6	OR2B11
3	OR2C1	OR2C3	OR2D2	OR2D3	OR2F1	OR2F2	OR2G2	OR2G3	OR2G6	OR2H1	OR2H2	OR2J2	OR2J3	OR2K2	OR2L2	OR2L3	OR2L5	OR2L8	OR2L13	OR2M2
4	OR2M3	OR2M4	OR2M5	OR2M7	OR2S2	OR2T1	OR2T2	OR2T3	OR2T4	OR2T5	OR2T6	OR2T7	OR2T8	OR2T10	OR2T11	OR2T12	OR2T27	OR2T29	OR2T33	OR2T34
5	OR2T35	OR2V1	OR2V2	OR2W1	OR2W3	OR2W5	OR2Y1	OR2Z1	OR2AE1	OR2AG1	OR2AG2	OR2AJ1	OR2AK2	OR2AP1	OR2AT4	OR3A1	OR3A2	OR3A3	OR3A4	OR4A5
6	OR4A15	OR4A16	OR4A47	OR4B1	OR4C3	OR4C5	OR4C6	OR4C11	OR4C12	OR4C13	OR4C15	OR4C16	OR4C45	OR4C46	OR4D1	OR4D2	OR4D5	OR4D6	OR4D9	OR4D10
7	OR4D11	OR4E2	OR4F4	OR4F5	OR4F6	OR4F15	OR4F16	OR4F17	OR4F21	OR4K1	OR4K2	OR4K5	OR4K13	OR4K14	OR4K15	OR4K17	OR4L1	OR4M1	OR4M2	OR4N2
8	OR4N4	OR4N5	OR4P4	OR4Q3	OR4S1	OR4S2	OR4X1	OR4X2	OR5A1	OR5A2	OR5B2	OR5B3	OR5B12	OR5B17	OR5B21	OR5C1	OR5D13	OR5D14	OR5D16	OR5D18
9	OR5F1	OR5H1	OR5H2	OR5H6	OR5H14	OR5H15	OR5I1	OR5J2	OR5K1	OR5K2	OR5K3	OR5K4	OR5L1	OR5L2	OR5M1	OR5M3	OR5M8	OR5M9	OR5M10	OR5M11
10	OR5P2	OR5P3	OR5R1	OR5T1	OR5T2	OR5T3	OR5V1	OR5W2	OR5AC2	OR5AK2	OR5AN1	OR5AP2	OR5AR1	OR5AS1	OR5AU1	OR6A2	OR6B1	OR6B2	OR6B3	OR6C1
11	OR6C2	OR6C3	OR6C4	OR6C6	OR6C65	OR6C68	OR6C70	OR6C74	OR6C75	OR6C76	OR6F1	OR6J2	OR6K2	OR6K3	OR6K6	OR6M1	OR6N1	OR6N2	OR6P1	OR6Q1
12	OR6S1	OR6T1	OR6V1	OR6X1	OR6Y1	OR7A5	OR7A10	OR7A17	OR7C1	OR7C2	OR7D2	OR7D4	OR7E24	OR7G1	OR7G2	OR7G3	OR8A1	OR8B2	OR8B3	OR8B4
13	OR8B8	OR8B12	OR8D1	OR8D2	OR8D4	OR8G1	OR8G5	OR8H1	OR8H2	OR8H3	OR8I2	OR8J1	OR8J3	OR8K1	OR8K3	OR8K5	OR8S1	OR8U1	OR8U8	OR8U9
14	OR9A2	OR9A4	OR9G1	OR9G4	OR9G9	OR9I1	OR9K2	OR9Q1	OR9Q2	OR10A2	OR10A3	OR10A4	OR10A5	OR10A6	OR10A7	OR10C1	OR10D3	OR10G2	OR10G3	OR10G4
15	OR10G6	OR10G7	OR10G8	OR10G9	OR10H1	OR10H2	OR10H3	OR10H4	OR10H5	OR10J1	OR10J3	OR10J5	OR10K1	OR10K2	OR10P1	OR10Q1	OR10R2	OR10S1	OR10T2	OR10V1
16	OR10W1	OR10X1	OR10Z1	OR10AD1	OR10AG1	OR11A1	OR11G2	OR11H1	OR11H2	OR11H4	OR11H6	OR11H12	OR11L1	OR12D2	OR12D3	OR13A1	OR13C2	OR13C3	OR13C4	OR13C5
17	OR13C8	OR13C9	OR13D1	OR13F1	OR13G1	OR13H1	OR13J1	OR14A2	OR14A16	OR14C36	OR14I1	OR14J1	OR14K1	OR51A2	OR51A4	OR51A7	OR51B2	OR51B4	OR51B5	OR51B6
18	OR51D1	OR51E1	OR51E2	OR51F1	OR51F2	OR51G1	OR51G2	OR51I1	OR51I2	OR51J1	OR51L1	OR51M1	OR51Q1	OR51S1	OR51T1	OR51V1	OR52A1	OR52A4	OR52A5	OR52B2
19	OR52B4	OR52B6	OR52D1	OR52E2	OR52E4	OR52E5	OR52E6	OR52E8	OR52H1	OR52I1	OR52I2	OR52J3	OR52K1	OR52K2	OR52L1	OR52M1	OR52N1	OR52N2	OR52N4	OR52N5
20	OR52R1	OR52W1	OR56A1	OR56A3	OR56A4	OR56A5	OR56B1	OR56B4												

Figure 5. OR Gene Arrangement for Visualization

(a) 20x20 matrix. ORs are designated in alphabetical order of the hORDE nomenclature. Cells without designated ORs are colored with black. (b) OR arrangement by OR family. (c) Subfamily arrangement of ORs

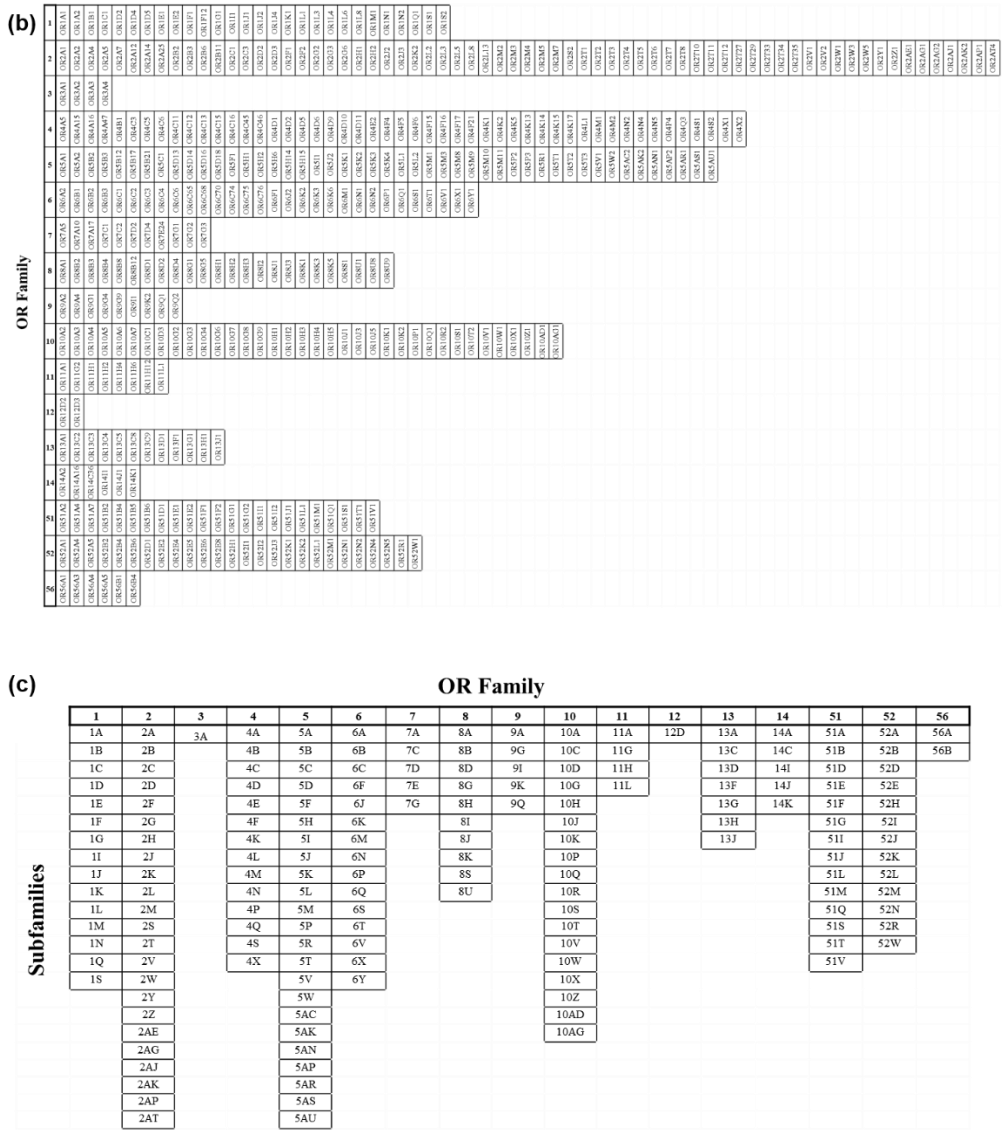

Figure 5. OR Gene Arrangement for Visualization

(a) 20x20 matrix. ORs are designated in alphabetical order of the hORDE nomenclature. Cells without designated ORs are colored with black. (b) OR arrangement by OR family. (c) Subfamily arrangement of ORs

3. Results

3.1. Heterologous expression of ORs

Heterologous expression of ORs on Hana3A cell surface was confirmed by western blot (Fig. 6). The sizes of ORs with Rho-tag and FLAG-tag are ranging from 35 to 40 kDa. The exact size of OR1A1 is 34.6 kDa. The housekeeping gene, β-actin, was detected to confirm the presence of cells transfected with the mock vectors. Later, it was demonstrated that the OR1A1 does not respond to any of three odorants (indole, methyl dihydrojasmonate, and naphthalene). This result suggests that the differences among the OR response levels were not driven by failure of the surface expression of ORs.

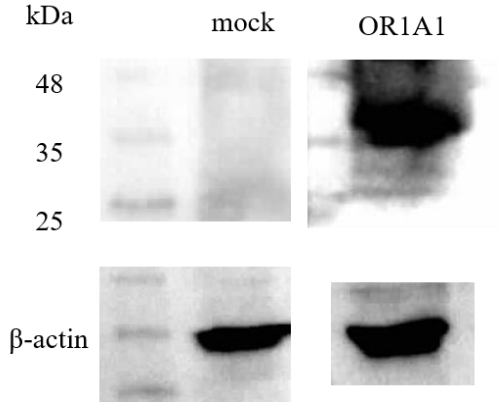

Figure 6. OR Expression on Hana3A Cells

OR1A1: 34.6 kDa, β-actin: ~40 kDa. Primary antibody: FLAG mouse mAb, β-actin mouse mAb. Secondary antibody: HRP-conjugated anti-mouse Ab.

3.2. Odorant cytotoxicity test

Cytotoxicity of three odorants to transfected Hana3A cells were measured (Fig. 7). The highest concentration that does not significantly affect the cell viability was indicated to be 100 μM for all three odorants. To minimize misunderstanding of OR responses due to low cell viability, 100 μM of odorants were used to select the responsive ORs.

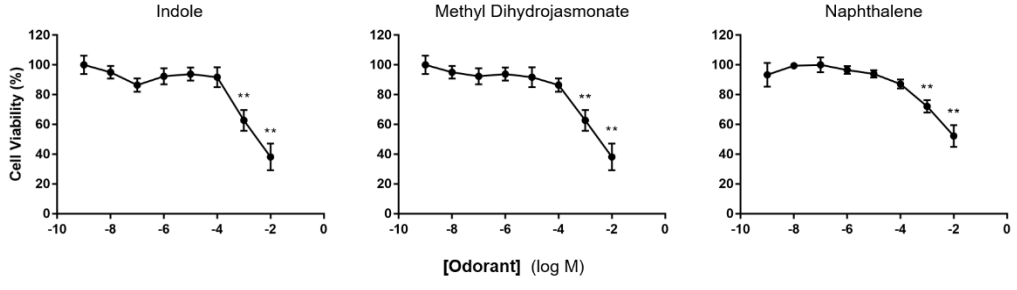

Figure 7. Cytotoxicity of Odorants on Hana3A Cells

The highest absorbance in each odorant was normalized to 100%, and 0 absorbance was normalized to 0%. n=6, * $p<0.05$, ** $p<0.01$

3.3. OR responses to indole

3.3.1. Selection of responsive ORs

The normalized luciferase activities in absence and presence of an odorant with six replicates were obtained. t-test was conducted to calculate p value between the two groups, and p values smaller than 0.05 were considered to be statistically significant. The ORs with significant increase of luciferase activity with odorant application were regarded to be activated by the odorant (Fig. 8; OR8B12).

52 ORs that positively respond to 100 μM of indole were selected (Fig. 9, Table 3). After the selection, response levels of the 52 ORs to 0 M, 1 μM, 10 μM, and 100 μM of indole were measured, and their sigmoidal curves were drawn (Fig. 10). This step was to confirm the positive correlation between the response levels of 52 ORs and indole concentrations and to determine the range for dose-response tests. 15 ORs with low response levels at 1uM of indole (medium sensitivity group) were tested with higher concentrations of indole (1 μM, 3 μM, 10 μM, 30 μM, 100 μM, 300 μM and 1 M) to obtain their EC_{50} values (Fig. 10b, 11b). 12 ORs only responded to 100 μM of indole (low sensitivity group, Fig. 10c). Their EC_{50} values were unmeasurable because of low cell viability at concentrations higher than 100 μM. Other than these 27 ORs, responsive ORs were stimulated with 1 nM, 10 nM, 100 nM, 1 μM, 10 μM, 100 μM and 1 mM of indole to obtain their sensitivities to indole (high sensitivity group, Fig. 10a, 11a).

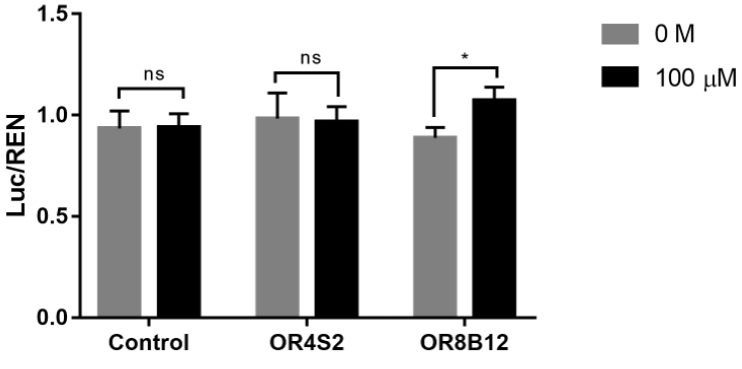

Figure 8. Normalized Luminescence Measurements

Luc/REN: normalized luciferase luminescence measurement, the ratio of firefly luciferase and *Renilla* luciferase. Luc: CRE promoter-mediated firefly luminescence, REN: *Renilla* luminescence, control: mock vector control, n=6, * $p<0.05$

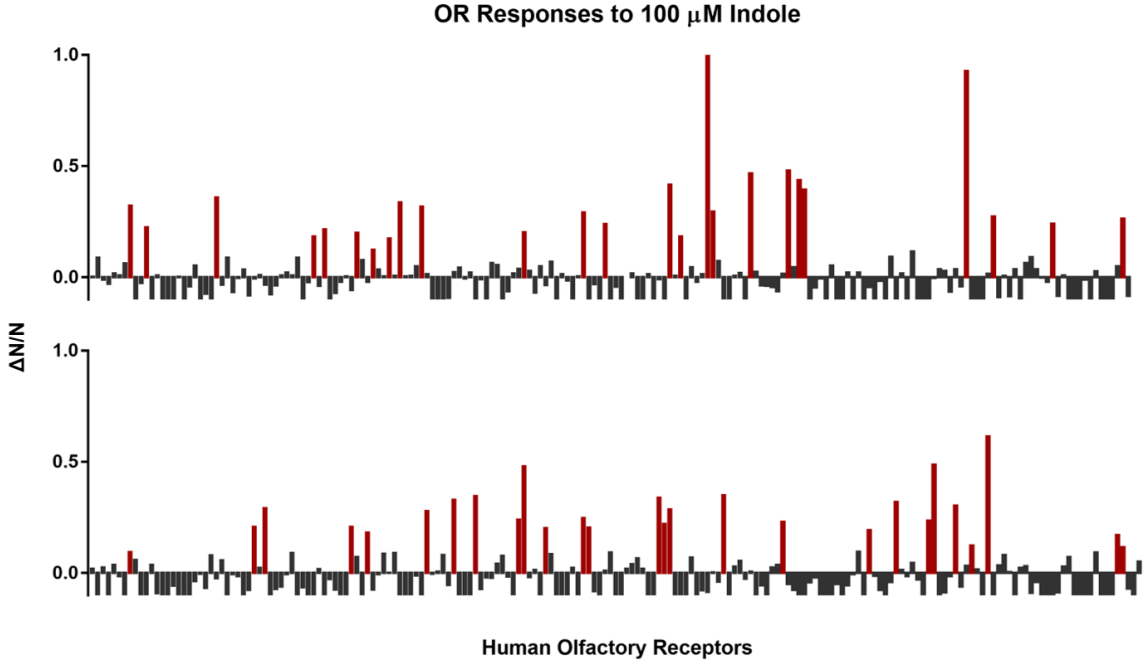

Figure 9. Normalized Luciferase Activities of 388 ORs in 100 μM Indole

ORs with statistically significant increases from the basal activity were selected and marked red.

ΔN/N: normalized luciferase activity ([N(odorant)-N(no-odorant)]/N(no-odorant)).

Table 3. Selection of 52 ORs That Positively Respond to 100 µM Indole

hORDE	Mean	ΔN/N	p value	hORDE	Mean	ΔN/N	p value
OR1D5	1.478	0.321	0.024	OR6V1	0.419	0.208	0.095
OR1F1	2.584	0.224	0.167	OR6Y1	1.154	0.290	0.095
OR1M1	2.274	0.358	0.024	OR8B12	1.072	0.207	0.024
OR2C1	3.195	0.184	0.167	OR8D4	1.160	0.180	0.167
OR2D2	0.948	0.215	0.048	OR8K5	1.721	0.277	0.024
OR2G6	1.509	0.200	0.024	OR9A2	3.265	0.329	0.024
OR2J2	2.250	0.124	0.024	OR9G9	0.915	0.345	0.048
OR2L2	2.043	0.303	0.048	OR10A5	0.847	0.238	0.048
OR2L5	0.583	0.337	0.095	OR10A6	1.131	0.481	0.024
OR2M3	1.749	0.318	0.024	OR10G2	0.538	0.201	0.095
OR2T34	1.134	0.202	0.143	OR10H1	1.433	0.247	0.024
OR2AG2	0.870	0.386	0.024	OR10H2	2.404	0.203	0.095
OR2AT4	0.643	0.238	0.024	OR10T2	0.940	0.338	0.024
OR4C6	1.474	0.417	0.024	OR10V1	1.383	0.103	0.167
OR4C12	0.783	0.143	0.024	OR10W1	1.025	0.384	0.024
OR4C46	0.819	0.456	0.036	OR11H6	0.985	0.350	0.024
OR4D1	0.768	0.170	0.095	OR13C9	0.758	0.230	0.095
OR4E2	0.644	0.468	0.167	OR51B4	0.881	0.193	0.048
OR4F21	0.752	0.481	0.143	OR51E2	20.802	0.319	0.024
OR4K2	0.823	0.437	0.048	OR51I2	1.616	0.235	0.036
OR4K5	2.382	0.394	0.048	OR51J1	1.543	0.488	0.024
OR5H1	3.029	0.928	0.024	OR51S1	1.045	0.303	0.024
OR5I1	1.244	0.272	0.024	OR52A1	0.695	0.123	0.167
OR5M9	1.451	0.241	0.095	OR52B2	1.446	0.614	0.024
OR5AN1	0.771	0.175	0.167	OR56A3	1.171	0.170	0.048
OR6C1	4.355	1.809	0.024	OR56A4	1.341	0.116	0.167

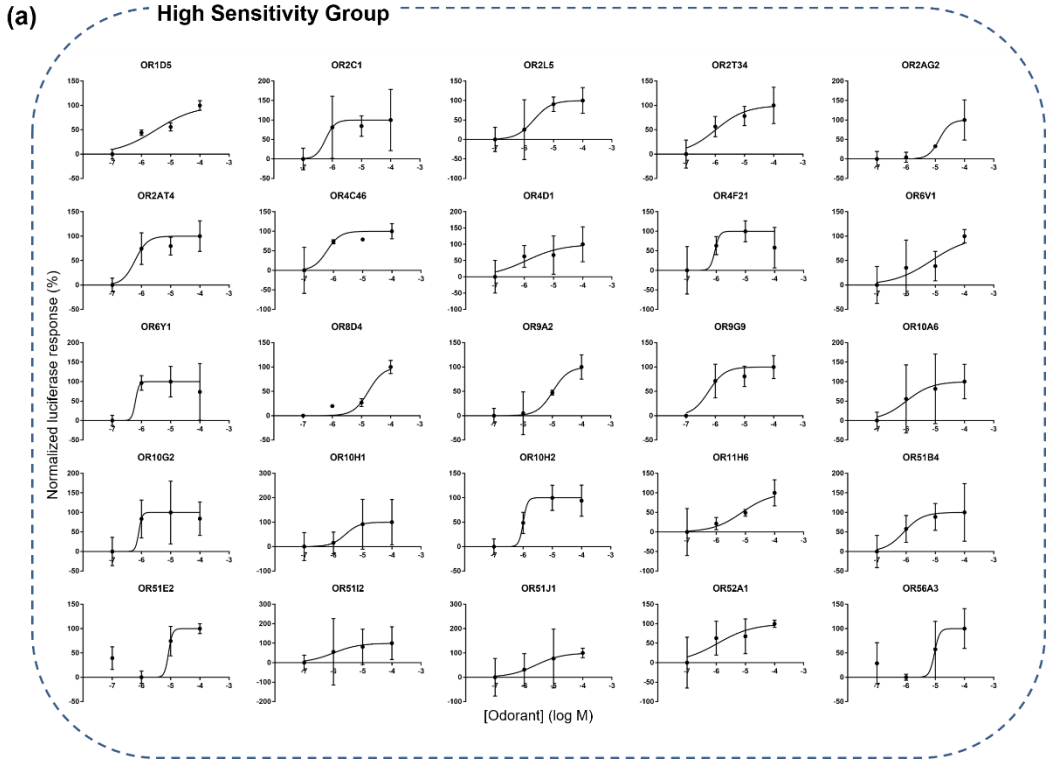

Figure 10. Normalized Response of the Receptors to 0 M, 1 μM, 10 μM and 100 μM of Indole

Normalized luciferase responses of selected 52 ORs at 4 different concentrations. (a) High sensitivity group of ORs that responded to 1 μM of indole. (b) The low sensitivity group with ORs that did not respond to 1 μM of indole. (c) The unmeasurable sensitivity group of ORs that only responded to 100 μM of indole. The lowest response, firefly / *Renilla*, of each OR was normalized to 0%, and the highest response was normalized to 100%. Error bars, s.e.m. over three replicates.

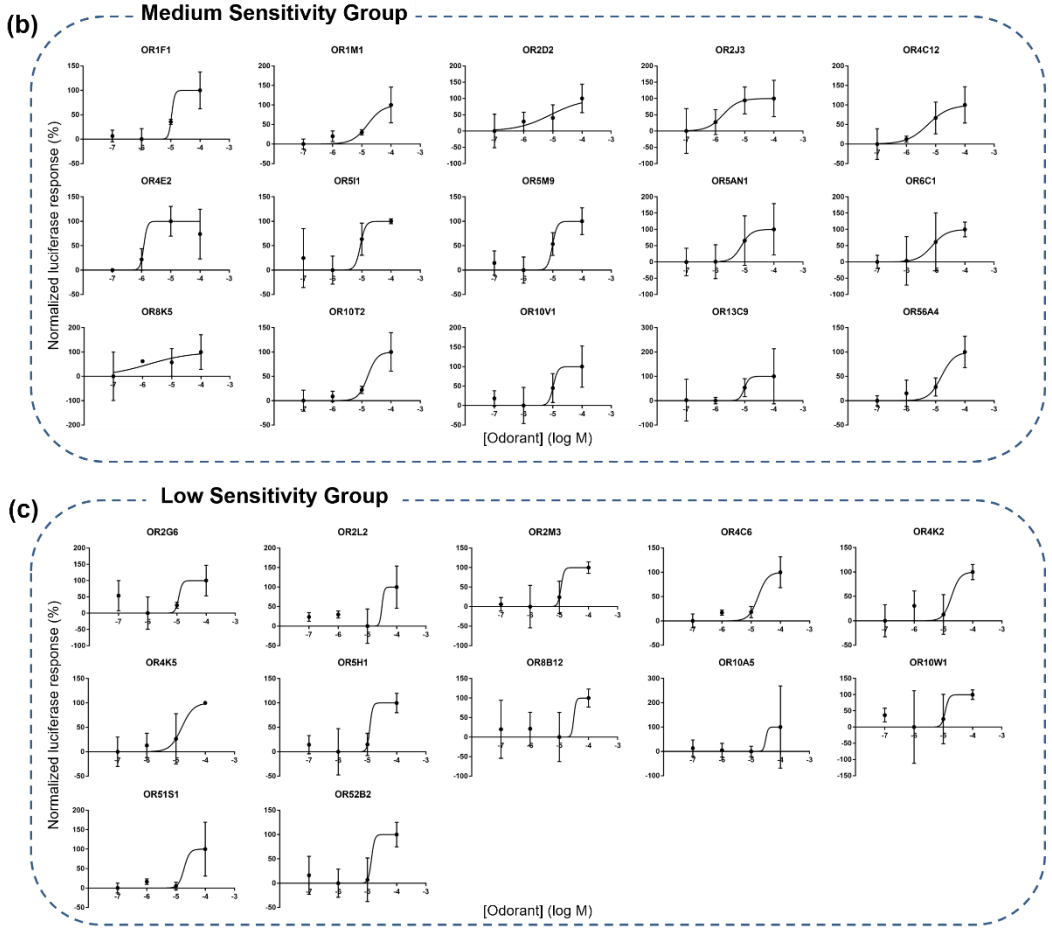

Figure 10. Normalized Responses of the Receptors to 0 M, 1 μM, 10 μM and 100 μM of Indole

Normalized luciferase responses of selected 52 ORs at 4 different concentrations. (a) High sensitivity group of ORs that responded to 1 μM of indole. (b) The low sensitivity group with ORs that did not respond to 1 μM of indole. (c) The unmeasurable sensitivity group of ORs that only responded to 100 μM of indole. The lowest response, firefly / *Renilla*, of each OR was normalized to 0%, and the highest response was normalized to 100%. Error bars, s.e.m. over three replicates.

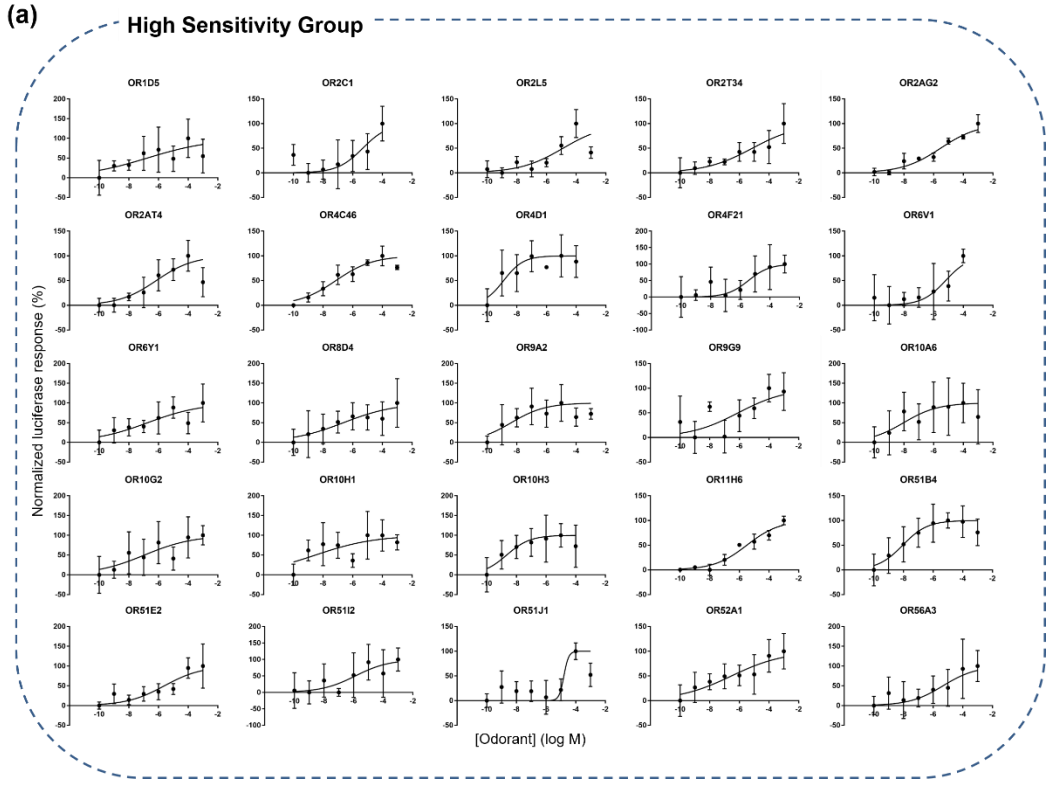

Figure 11. Normalized Dose-Response Curves for 40 ORs to Indole

Each group was tested with a different set of concentration range. (a) The high sensitivity group stimulated with indole ranging from 1 nM to 1mM. (b) The low sensitivity group stimulated with indole ranging from 1 μM to 1mM.The lowest normalized luciferase luminescence measurements (Luc / Ren) of each OR was normalized to 0%, and the highest response was normalized to 100%. Error bars, s.e.m. over six replicates.

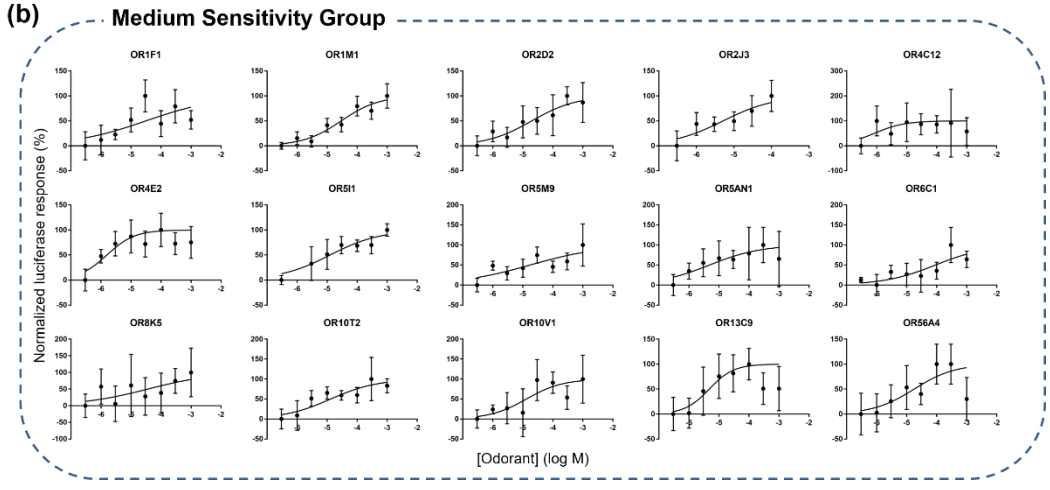

Figure 11. Normalized Dose-Response Curves for 40 ORs to Indole

Each group was tested with a different set of concentration range. (a) The high sensitivity group stimulated with indole ranging from 1 nM to 1mM. (b) The low sensitivity group stimulated with indole ranging from 1 μM to 1mM.The lowest normalized luciferase luminescence measurements (Luc / Ren) of each OR was normalized to 0%, and the highest response was normalized to 100%. Error bars, s.e.m. over six replicates.

3.3.2. Visualization

The response patterns of ORs were visualized on heatmaps. The representative response pattern of indole was displayed using the sensitivities of ORs to indole (Fig. 12). Visualization on a 20x20 matrix allows analysis and comparison between two patterns (Fig. 12a). Considering that ORs with similar protein sequences have aspects of interacting with structurally similar ligands [2], the overall response patterns were also visualized according to the OR families (Fig. 12b).

In addition, OR response patterns at different concentrations of indole were visualized (Fig. 13). The number of responsive ORs and their response intensities positively correlated with the indole concentration. About 10 ORs additionally responded when indole concentration increased by 10 times. The number of responsive ORs increased the greatest (14 ORs) when the indole concentration increased from 10 μM to 100 μM.

To compare the patterns between different odorants on the subfamily level, the response patterns to indole at different concentrations were also visualized according to their subfamilies. The fraction of responsive ORs per subfamily was used. Thus, this method excluded the information of the response intensities of individual ORs and only focused on the types and number of ORs.

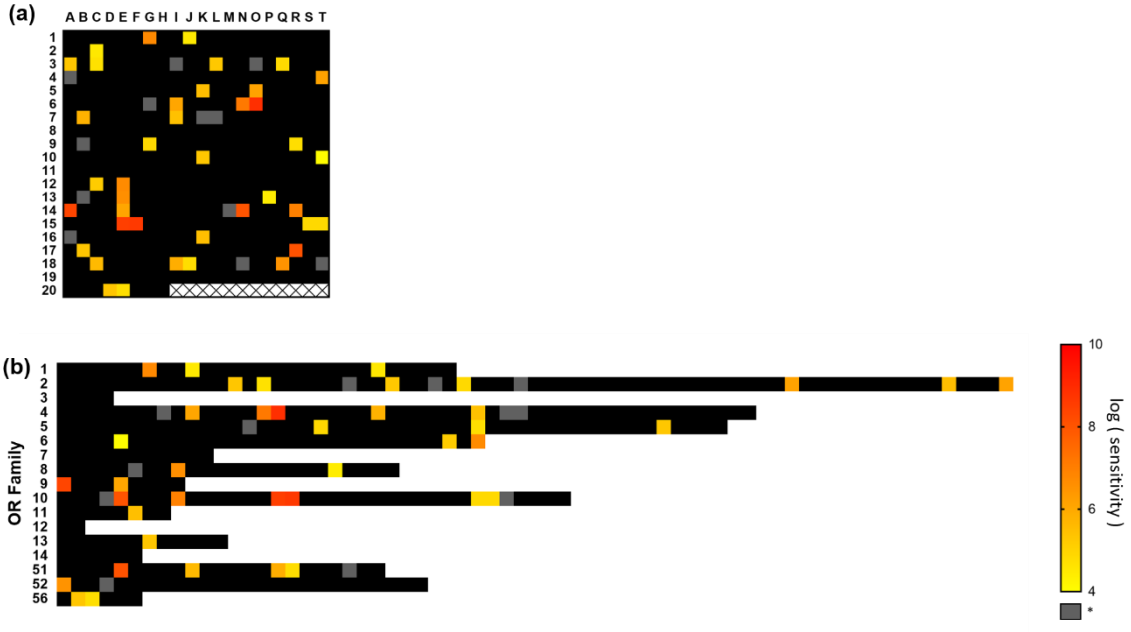

Figure 12. Overall Response Patterns of ORs to Indole

(a) 20 x 20 heatmap matrix of the overall response pattern of ORs to indole. Number and alphabet labels are for matrix cell representation. Cells with X are blanks without designates ORs. (b) OR family based heatmap display of overall response pattern of ORs to indole. The number titles show the names of OR families. The logarithm of the sensitivity, $\log(1/EC_{50})$, of each OR is used. Cells with ORs that have EC_{50} out of the measurable range are colored grey.

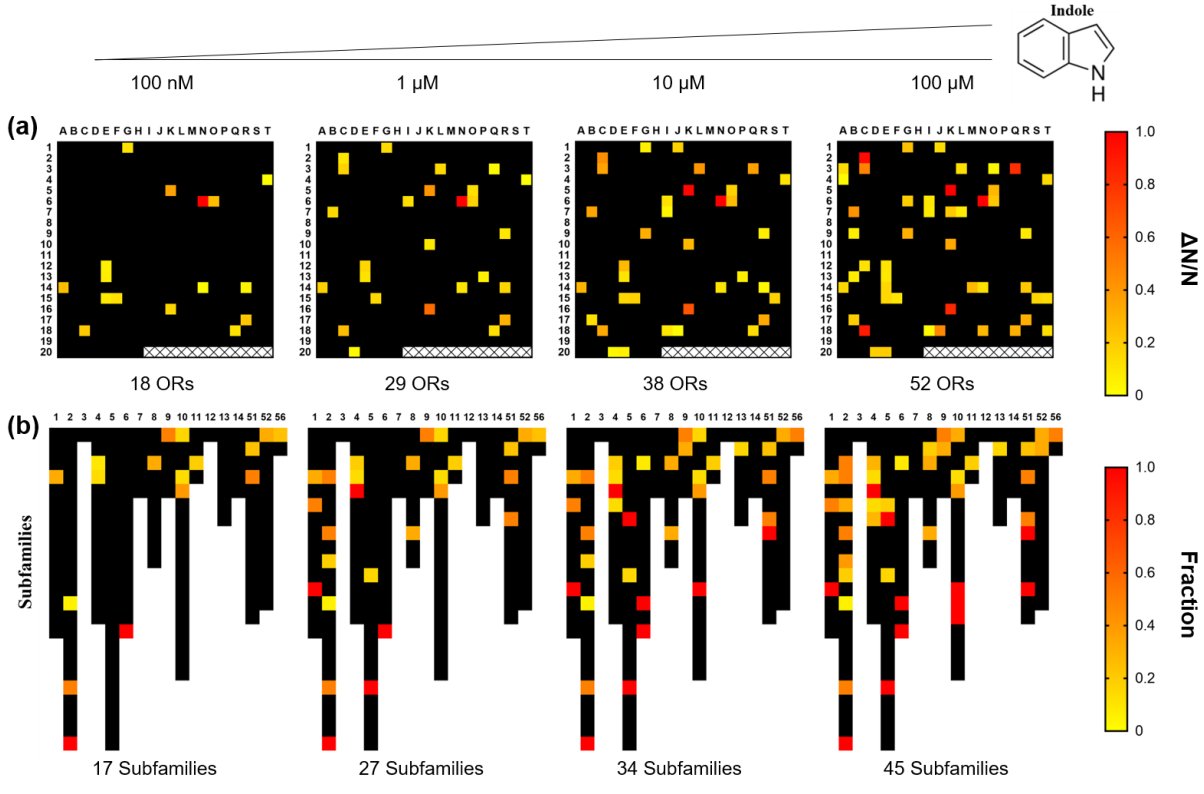

Figure 13. Response Patterns of ORs at Different Concentrations of Indole

(a) Response patterns of ORs to different concentrations of indole. Each cell indicates normalized response of the designated OR such that ΔN/N. (b) Heatmap display of responding OR fractions of subfamilies at different concentrations of indole. Number labels of columns are OR family names. Each cell represents a subfamily, and the fraction of positively responding ORs of each subfamily was used.

3.4. OR responses to methyl dihydrojasmonate and naphthalene

3.4.1. Selection of responsive ORs

Response levels of 388 ORs to 100 μM methyl dihydrojasmonate and 100 μM naphthalene were measured (Fig. 14). ORs whose response values in odorants were significantly higher than that in absence of odorants ($p<0.05$) were considered to be responsive. 36 ORs responded to 100 μM methyl dihydrojasmonate (Fig. 14a, Table 4), and 60 ORs responded to 100 μM of naphthalene (Fig. 14b, Table 5).

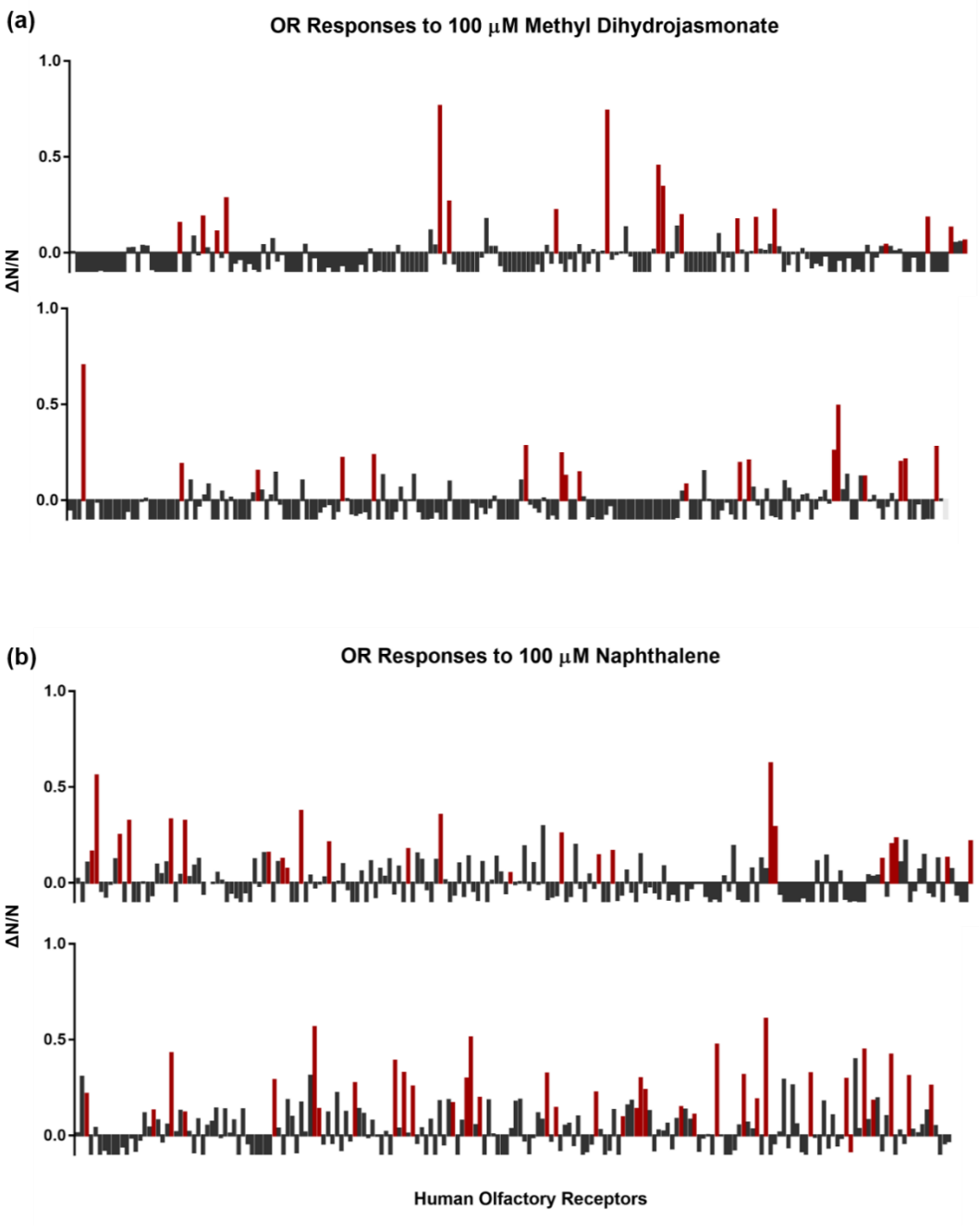

Figure 14. Normalized Luciferase Activities

ΔN/N in (a) 100 μM methyl dihydrojasmonate and (b) 100 μM naphthalene.

Table 4. Selection of 36 ORs That Positively Respond to 100 µM Methyl Dihydrojasmonate

hORDE	Mean	ΔN/N	p value	hORDE	Mean	ΔN/N	p value
OR1M1	0.896	0.156	0.024	OR6A2	0.683877	0.704309	0.0238
OR1S2	1.117	0.188	0.036	OR6N2	1.123394	0.189298	0.0476
OR2A4	0.767	0.110	0.036	OR7G2	0.798086	0.153989	0.0043
OR2A7	1.158	0.284	0.032	OR8K1	2.352029	0.221214	0.0238
OR2T33	2.507	0.766	0.004	OR9A2	1.210736	0.236202	0.0317
OR2T35	3.129	0.268	0.029	OR10P1	2.739687	0.281411	0.0476
OR4B1	1.056	0.222	0.024	OR10Z1	1.290025	0.243735	0.0357
OR4D1	0.493	0.742	0.036	OR10AD1	0.523354	0.126573	0.0238
OR4F15	1.384	0.454	0.048	OR11G2	2.432334	0.14506	0.0357
OR4F16	1.261	0.344	0.036	OR14I1	1.488213	0.083304	0.0357
OR4K2	0.448	0.197	0.024	OR51E2	17.48138	0.195047	0.0238
OR4P4	1.251	0.173	0.032	OR51F2	1.225757	0.20826	0.0159
OR4X1	1.444	0.181	0.048	OR52E2	1.423209	0.257503	0.0317
OR5B2	0.510	0.225	0.024	OR52E4	0.576822	0.493042	0.0357
OR5M1	1.116	0.079	0.036	OR52I1	1.170471	0.123705	0.0476
OR5T1	0.453	0.184	0.048	OR52N2	1.444356	0.199349	0.0357
OR5AC2	1.979	0.132	0.048	OR52N4	0.611038	0.21213	0.0476
OR5AP2	1.206	0.064	0.048	OR56A5	0.468044	0.277949	0.0357

Table 5. Selection of 60 ORs That Positively Respond to 100 µM Naphthalene

hORDE	Mean	ΔN/N	p value
OR1B1	0.162	0.563	0.024
OR1C1	0.560	1.297	0.024
OR1E2	0.250	1.068	0.024
OR1F12	0.323	0.444	0.024
OR1L4	0.330	0.945	0.024
OR1M1	0.323	1.572	0.024
OR2C1	0.157	2.633	0.036
OR2D3	0.125	0.533	0.048
OR2F1	0.074	1.933	0.036
OR2G3	0.376	1.525	0.024
OR2K2	0.211	0.911	0.048
OR2T6	0.176	0.974	0.048
OR2T29	0.355	0.984	0.024
OR2AK2	0.050	1.008	0.048
OR4B1	0.258	2.838	0.024
OR4C16	0.144	0.576	0.024
OR4D1	0.167	2.124	0.024
OR5A1	0.624	2.243	0.024
OR5A2	0.292	1.248	0.024
OR5L1	0.125	0.844	0.024
OR5M1	0.203	0.769	0.024
OR5M3	0.232	0.856	0.024
OR5V1	0.130	0.552	0.026
OR5AP2	0.217	0.692	0.024
OR5AU1	0.216	2.843	0.024
OR6C76	0.131	0.386	0.024
OR6K3	0.428	2.121	0.024
OR6N1	0.119	1.488	0.048
OR8A1	0.289	2.708	0.024
OR8G1	0.565	13.575	0.008
OR8G5	0.138	0.692	0.024
OR8K3	0.273	0.988	0.048
OR9G4	0.390	0.595	0.024
OR9I1	0.327	1.399	0.024
OR9Q1	0.255	1.933	0.024
OR10D3	0.168	0.912	0.024
OR10G4	0.297	1.248	0.024
OR10G6	0.512	0.606	0.024
OR10G8	0.196	1.421	0.024
OR10S1	0.323	1.130	0.024
OR10V1	0.145	0.860	0.048
OR11H2	0.224	0.761	0.024
OR12D3	0.096	1.296	0.002
OR13C3	0.139	0.456	0.048
OR13C4	0.299	1.346	0.024
OR13C5	0.236	0.969	0.024
OR14A2	0.148	1.350	0.024
OR14I1	0.109	1.338	0.048
OR51A7	0.473	0.887	0.024
OR51E1	0.316	0.835	0.024
OR51F2	0.189	1.172	0.024
OR51G2	0.608	0.967	0.048
OR52A1	0.324	1.098	0.024
OR52E5	0.294	0.885	0.024
OR52E6	0.397	1.326	0.024
OR52H1	0.447	1.360	0.024
OR52I2	0.180	0.796	0.048
OR52L1	0.421	0.923	0.024
OR52N4	0.310	0.880	0.024
OR56A3	0.260	0.588	0.036

3.4.2. Visualization

The OR response patterns in methyl dihydrojasmonate and naphthalene were visualized on 20x20 matrices and according to their subfamilies (Fig. 15). Because the response levels were measured only at one concentration (100 μM), EC_{50} values were unavailable to build the overall response patterns.

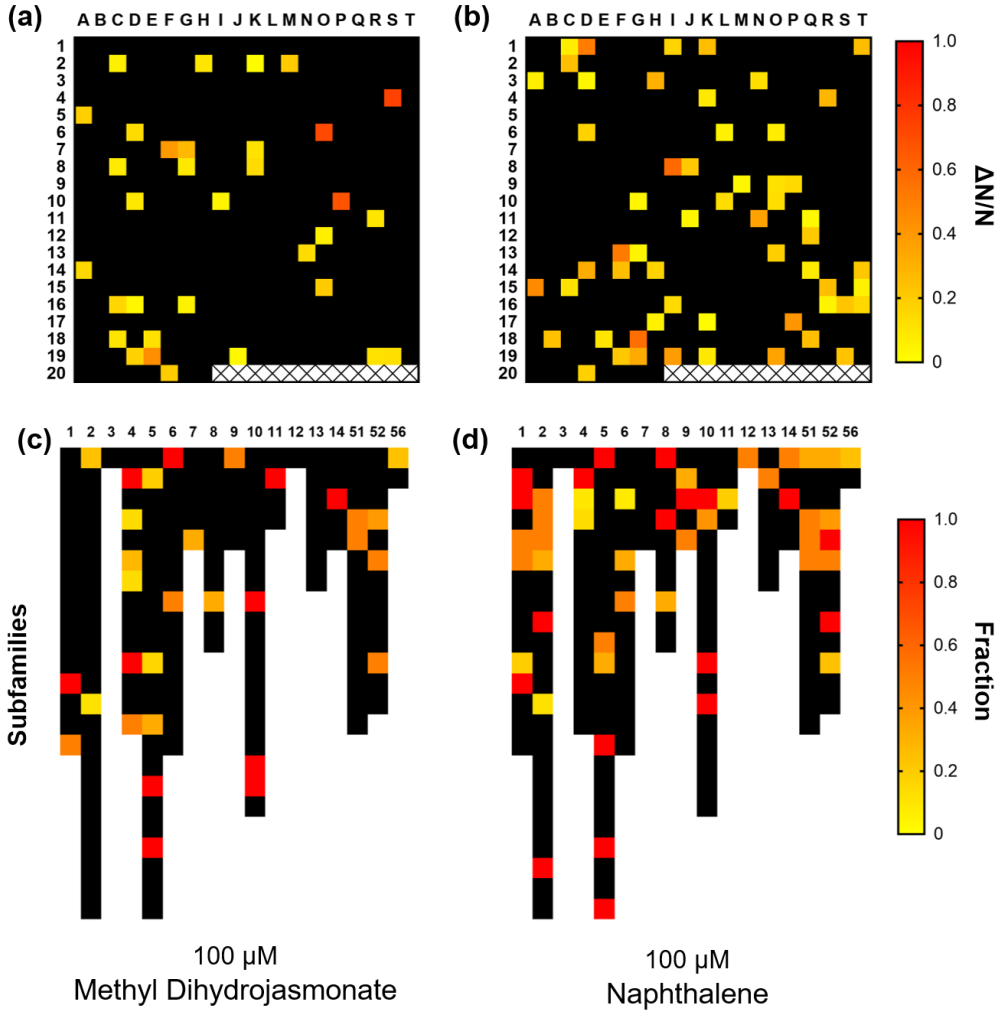

Figure 15. Response Patterns of ORs to Methyl Dihydrojasmonate and Naphthalene

(a), (b) 20 x 20 heatmap matrices of OR response patterns. (c), (d) Heatmaps of responding OR fractions of subfamilies. (a), (c) Responses to 100 μM methyl dihydrojasmonate. (b), (d) Responses to 100 μM naphthalene.

3.5. Pattern comparison

3.5.1. Pattern comparison

There was a positive correlation between the odor strength and the number of responsive ORs. Strength of perceived smell is weakest for methyl dihydrojasmonate and strongest for naphthalene. The number of responsive ORs were also smallest for 100 μM methyl dihydrojasmonate (36 ORs, Table 4, Fig. 15), then 100 μM indole (52 ORs, Table 3, Fig. 13) and greatest for 100 uM naphthalene (60 ORs, Table 5, Fig. 15). The normalized response levels were not high (red) for naphthalene while indole and methyl dihydrojasmonate contained several ORs with high normalized response levels (Fig. 15)

3.5.2. Comparison of responsive ORs

ORs responding to low and high concentrations (100 nM, 100 μM) of indole were compared with 100 μM methyl dihydrojasmonate and 100 μM naphthalene. The ORs that respond to both of the odorants were listed (Table 6). The number of matching ORs was not dependent on the odor similarity of odorants but correlated with the odorant concentration.

It was found that OR1M1 and OR4D1 reacted to all three odorants so are likely to be broadly tuned receptors. OR1M1 responded to three odorants when the concentrations of odorants were high (100 μM). OR4D1 had more sensitivity to indole than OR1M1 as it was activated by 100 nM of indole.

The response intensities of the matching ORs were compared (Fig. 16). The intensities of matching ORs between indole and methyl dihydrojasmonate did not correspond and

had little similarity regardless of the concentrations of indole. In contrast, those of matching ORs between 100 μM indole and naphthalene showed similar intensity values.

Table 6. ORs That Respond to Both of the Compared Odorants

Indole - Methyl Dihydrojasmonate

	Indole 100 nM	Methyl Dihydrojasmonate 100 µM
hORDE	ΔN/N	ΔN/N
OR4D1	0.331	0.742
OR9A2	0.329	0.236
OR51E2	0.280	0.195
No. of matching ORs	3	
Matching %	16.7%	8.3%

	Indole 100 µM	Methyl Dihydrojasmonate 100 µM
hORDE	ΔN/N	ΔN/N
OR1M1	0.966	0.156
OR4D1	0.295	0.742
OR4K2	0.288	0.197
OR9A2	0.232	0.236
OR51E2	0.907	0.195
No. of matching ORs	5	
Matching %	9.6%	13.9%

Indole - Naphthalene

	Indole 100 nM	Naphthalene 100 µM
hORDE	ΔN/N	ΔN/N
OR4D1	0.331	0.167
OR52A1	0.204	0.324
OR56A3	0.055	0.260
No. of matching ORs	3	
Matching %	16.7%	5%

	Indole 100 µM	Naphthalene 100 µM
hORDE	ΔN/N	ΔN/N
OR1M1	0.966	0.323
OR2C1	0.217	0.157
OR4D1	0.295	0.167
OR10V1	0.221	0.145
OR52A1	0.376	0.324
OR56A3	0.269	0.260
No. of matching ORs	6	
Matching %	11.5%	10.0%

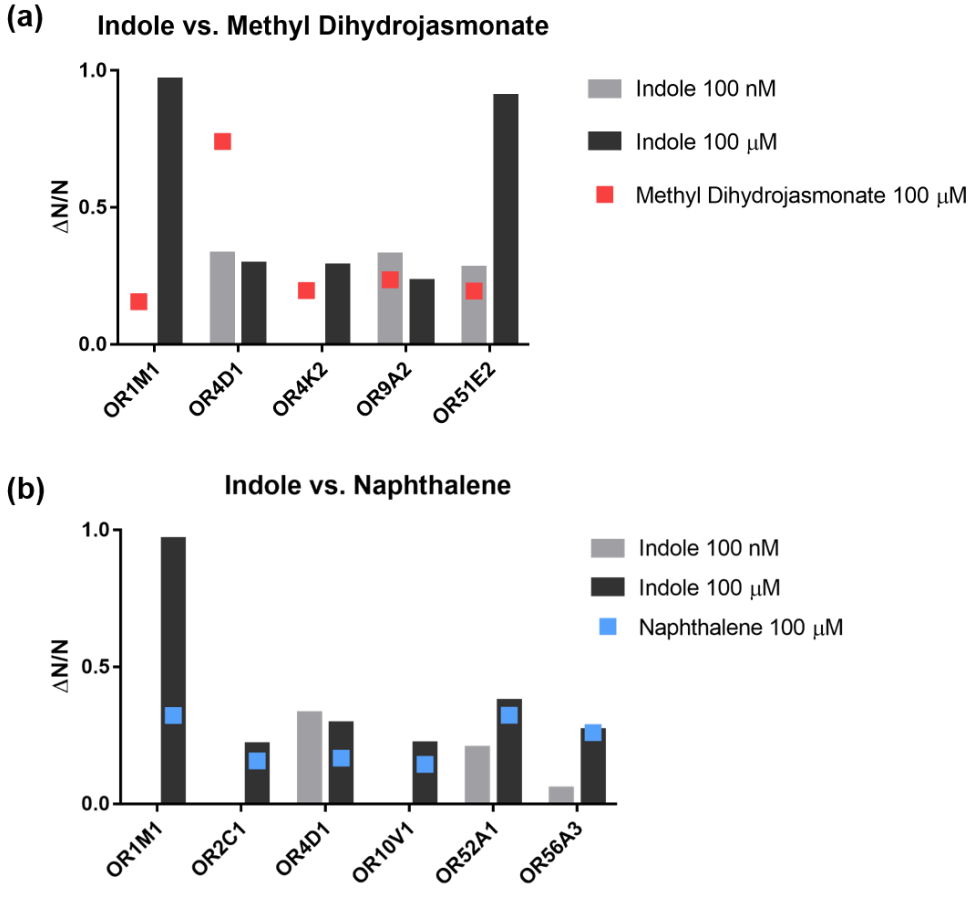

Figure 16. Response Intensities of Matching ORs

Response intensities of ORs that commonly responded to (a) indole (100 nM and 100 μM) and methyl dihydrojasmonate (100 μM) and (b) indole (100 nM and 100 μM) and naphthalene (100 μM).

3.5.3. Comparison of responsive OR subfamilies

The number of responsive ORs was insufficient to understand the odor similarity on the individual OR protein level. However, it was noticed that the matching ORs between indole and methyl dihydrojasmonate and those between indole and naphthalene did not share a single subfamily. This result and the evidence of relation between receptor protein sequence similarity and affinity to structurally similar ligands [2] suggested that OR subfamilies may have sufficient specificity to distinguish and compare the response patterns to different odorants. To demonstrate this, the OR response patterns were compared at the subfamily level (Fig. 17). The response patterns on the subfamily level were unique and distinguishable. The numbers of matching subfamilies were much greater than that of matching ORs between two odorants.

The number of subfamilies responding to indole increased by 28, from 17 to 45, when the indole concentration increased from 100 nM to 100 μM. The number of matching subfamilies between indole and naphthalene increased by 10 with the indole concentration increased. This increase ratio was twice of that between indole and methyl dihydrojasmonate (Fig. 18, Table 7). According to the number of matching subfamilies between odorants, the response pattern to indole became more similar with that of naphthalene than that of methyl dihydrojasmonate.

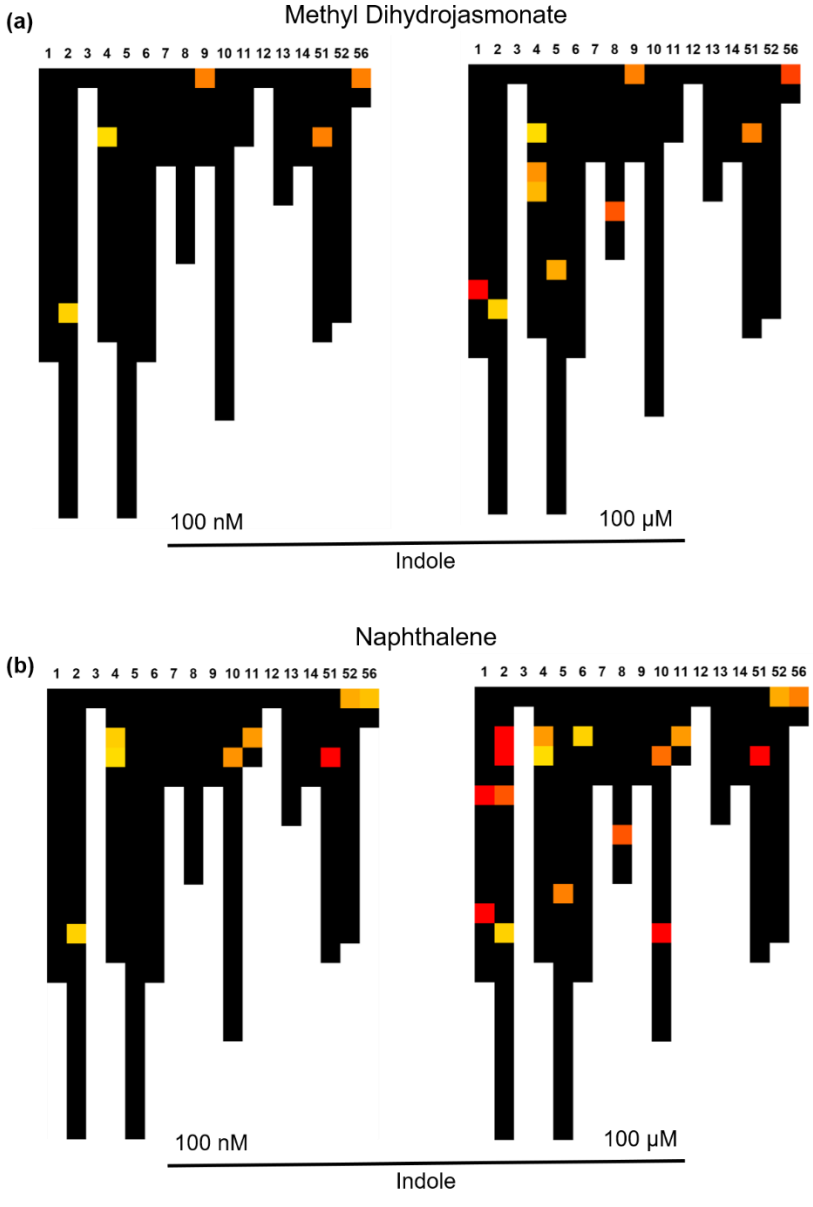

Figure 17. Fractions of ORs in Subfamilies Responding to Both of the Compared Odorants

(a) Comparison between 100 µM naphthalene and indole at 100 nM (left) and 100 µM (right). (b) Comparison between 100 µM methyl dihydrojasmonate and indole at 100 nM (left) and 100 µM (right).

Table 7. OR Subfamilies That Respond to Both of the Compared Odorants

	Indole 100 nM	Methyl Dihydrojasmonate 100 μM	Indole 100 μM	Methyl Dihydrojasmonate 100 μM
No. responding subfamilies	17	29	45	29
No. matching subfamilies	5		10	
% matching	29.4%	17.2%	22.2%	34.5%

	Indole 100 nM	Naphthalene 100 μM	Indole 100 μM	Naphthalene 100 μM
No. responding subfamilies	17	51	45	51
No. matching subfamilies	8		18	
% matching	47.1%	15.7%	40.0%	35.3%

% matching: (No. matching subfamilies)/(No. responding ORs)*100

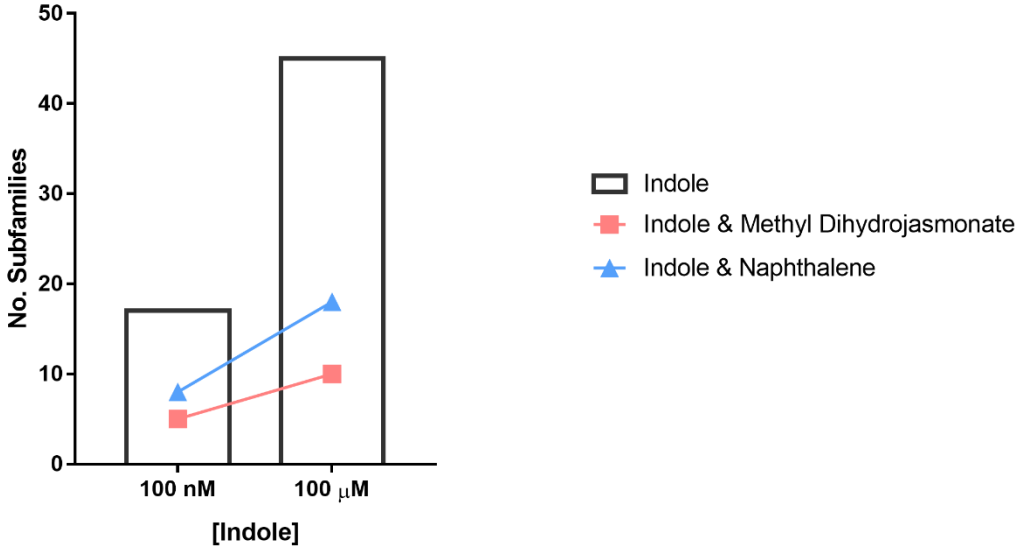

Figure 18. Increase of the Number of Matching Subfamilies Between Different Odorants

The bar graph indicates the number of responsive subfamilies at the given concentration of indole. The red plots indicate the number of matching OR subfamilies between 100 μM methyl dihydrojasmonate and the given concentration of indole. The blue plots are the number of matching subfamilies between 100 μM naphthalene and the given concentration of indole.

4. Discussion

4.1. Power-law distribution and inverse agonism

At the OSN level, OSN response sensitivity and intensity follow a power-law distribution [32, 33]. This allowed us to assume that ORs that do not respond to an odorant at high concentration would not respond to the odorant at lower concentration. The dose-response curves of responsive ORs showed that the response levels of ORs increased with the odorant concentration and were fit onto sigmoidal curves which supports the assumption.

Additionally, OSNs have different basal activities, and some odorants work as inverse agonists that reduce the response level below the basal activity [34, 35]. There are reports that some odorous molecules act as inverse agonists to ORs, and aromatic compounds are likely to show this tendency [36]. In this study, some ORs also showed decreased luciferase activity by indole than when no odorant was applied (Fig. 9; negative values). How the inverse agonism of molecules to ORs affect the odor perception is unknown, and it has been suggested that the inverse agonism may work to direct axonal targeting of OSN rather than the odor perception [37]. Because the OR response level was measured in vitro, it is not certain if the decrease in response level was because of inverse agonism. In fact, it is supposed that the decreases and different basal activities of ORs may be due to compromised overall cell viability with certain ORs [20]. In this study, we only focused on the ORs that odorants work as agonists. The function of inverse agonism on odor perception needs to be studied to further understand the odor perception mechanism.

4.2. Strength of smell, the number of responsive ORs and response intensity

The strength of perceived smell is the weakest for methyl dihydrojasmonate then indole and the strongest for naphthalene. The number of responsive ORs to the same concentration (100 μM) of three odorants showed a positive correlation with the smell strength (Fig. 13, 15). This suggests that the strength smell may refers to a large number of types of neurons activated by the odorants, not the perception based on the specific response patterns of ORs.

It was also supposed that the strength of odor may be due to the response intensities of ORs to certain odorants. However, it was found that the intensities of responses to naphthalene, which has the strongest smell, did not have normalized response levels higher than 0.7 (displayed with red color). In contrast, the odorants with weaker smell, indole and methyl dihydrojasmonate, had several responsive ORs with normalized activity higher than 0.7. It cannot be concluded if the strength of smell depends on the response intensity of ORs to an odorant because different OR types have different expression levels in nasal mucus [38]. Therefore, there is a possibility that weakly responding ORs in this heterologous system actually deliver much stronger signals to the OB. However, the individual ORs themselves did not strongly respond to odorants with strong odors.

4.3. Intensity difference of a same OR to different odorants

Even though it is impossible to compare the response intensities among different ORs due to different expression levels of ORs, it was possible to compare the intensity of a same OR to different odorants (Table 6). The intensities of matching ORs were distinct between indole and methyl dihydrojasmonate. In contrast, those between indole and naphthalene were much closer (Fig. 16). Different intensities of an OR to different odorants on the pattern refers to different sensitivities of the OR to the odorants. In contrast, similar intensities to odorants indicate that the OR lies on similar sigmoidal curves and have similar sensitivities against different odorants. Greater similarity between structurally similar odorants (indole and naphthalene) than that between structurally distant odorants (indole and methyl dihydrojasmonate) demonstrates that an OR has higher similarities to structurally close odorants than distant odorants.

4.4. Response patterns of OR subfamilies

The number of matching subfamilies indicated that the similarity between patterns increased more between indole and naphthalene than that between indole and methyl dihydrojasmonate with increase of indole concentration (Fig. 18). Reminding that the perceived smell of indole at high concentration is much closer to naphthalene than methyl dihydrojasmonate, it suggests that differences and similarity of response patterns at the subfamily level may be sufficient to decide the odor perception. It is also supposed that little differences in the protein sequences may allow detection of odorants with similar structure.

4.5. OR response patterning

The overall response patterns of ORs especially measured in a heterologous system must be very different from the signal patterns that olfactory cortex receives because of four reasons. First, the heterologous system does not include any of the enzymatic reactions occurring in nasal mucus. There are enzymes in human nasal mucus that catalyze certain odorous molecules, and their reactions drive different odor perception [39, 40, 41]. The complete list of mucosal enzymes is not established, and there are enzyme variations between individuals. It is also very difficult to build the mucosal environment in vitro. Therefore, we excluded all the enzymatic reactions and other obstruction and only considered the direct interactions between ORs and the odorous molecules. Second, the expression level of ORs differ by their types in nasal mucus. This expression ratio is not yet well known and varies by individuals. Therefore, we normalized the OR expression level with the number of cells and transfection efficiency. This may derive gaps between intensity of response in the heterologous system and the actual intensity processed in the human olfactory system. Therefore, the intensity differences among ORs on the coded patterns do not represent the actual differences of intensities sent along the OSNs. Next, the OR genes have large variations between individuals [18, 42, 43]. There are lots of SNPs that affect the OR sequences among races and individuals, and the differences affect the odor interpretation. We ignored the genetic variations, and the secured OR gene library minimized the genetic variations between experimental trials. Lastly, signals delivered by OSNs are processed before they are interpreted by the olfactory cortex. It was demonstrated that the input and output patterns at OB lie of different dimensions and

become more complicated by obtaining higher dimensionality as being processed [44]. Lots of efforts to screen the olfactory signals on the neuronal level have been made [45, 46, 47]. However, methods for OSN pattern screening in human OB in vivo are unavailable. Furthermore, olfaction is a very subjective sense, so the perception of smell can be affected by experiential and environmental conditions.

Because of the complexity of olfaction, standardization that excludes the individual variations and subjectivity is important. This patterning method has assumptions such that the OR expression levels are identical, no enzymatic reactions occur, no antagonism between odorous molecules occurs, and there are no genetic variations of OR genes. Prediction of smell with the OR response pattern is yet very difficult due to the large differences between the experimental patterns and the actual patterns. However, the patterning of smell that exclude the variations will assist to record smell, and it will contribute to the standardization of olfaction and further understanding of sense of smell.

5. Conclusions

Olfaction is driven by very complicated mechanisms involving processes through olfactory receptors, sensory neurons, the olfactory bulb and the olfactory cortex. The smell perception is also strongly affected by individual experiences, environment and subjectivity. Due to its complexity, olfaction is still the most unknown sense among the five basic senses.

This study suggests a visualization method to represent smell in terms of sensitivities and response levels of 388 ORs to a given odor. For encoding of smell, 388 functional human ORs were inserted into pcDNA3.0 vectors and cloned. A heterologous system that imitates the olfactory receptor response mechanism was used. The cAMP was produced when heterologously expressed ORs bind to the applied odorant just as OSN in the intrinsic olfactory system, and the cAMP level was used to measure the response levels of ORs. Using this system, the response levels of 388 ORs to three odorants that have similarity and differences in terms of the perceived odor description and chemical structures.

It was found that the number of responsive ORs and their response intensity levels corresponded to the odorant concentration. A positive correlation between the strength of odor and the number of responsive ORs was found. Additionally, the relation between similarity of molecular structures of odorants and OR sensitivities to the odorants was demonstrated. The results also suggested that analysis of response patterns at OR subfamily level may be sufficient to distinguish and understand the odors.

Even though there were several relations between similar odors and OR response patterns, it was not sufficient to predict and interpret odors by their response patterns. This result confirms high specificity of ORs and suggests that an OR-based electrical nose must have much greater sensitivity and accuracy to distinguish and recognize odorants. OR-based sensors will be able to recognize target chemicals with much greater sensitivity and accuracy than animal-based detection.

Furthermore, visualization of olfaction will allow accurate analysis and comparison of odors at the OR level. The in vitro olfactory system that excludes personal interpretation and biological variations will provide more objective environment to record odors. This method to code and record odors will contribute to standardization of olfaction, establishment of OR-based biosensors, and further understanding of olfaction.

6. Reference

1. Glusman, G., Yanai, I., Rubin, I., & Lancet, D. (2001). The complete human olfactory subgenome. *Genome Research*, 11(5), 685–702.
2. Malnic, B., Godfrey, P. A., & Buck, L. B. (2004). The human olfactory receptor gene family. *Proceedings of the National Academy of Sciences of the United States of America*, 101(8), 2584–2589.
3. Firestein, S. (2001). How the olfactory system makes sense of scents. *Nature*, 413, 211–218.
4. Reed RR. (1990) How does the nose know? *Cell* 60, 1–2
5. Linda, B., & Richard Axel. (1991). A Novel Multigene Family May Encode Odorant Receptors: A Molecular Basis for Odor Recognition. *Cell*, 65, 175–187.
6. Malnic, B., Hirono, J., Sato, T., & Buck, L. B. (1999). Combinatorial receptor codes for odors. *Cell*, 96(5), 713–723.
7. Lancet D, Pace U (1987) The molecular basis of odor recognition. *Trends Biochem Sci* 12, 63–66
8. Glusman, G., Bahar, A., Sharon, D., Pilpel, Y., White, J., & Lancet, D. (2000). The olfactory receptor gene superfamily: Data mining, classification, and nomenclature. *Mammalian Genome*, 11(11), 1016–1023.
9. Olender, T., Lancet, D., & Nebert, D. W. (2008). Update on the olfactory receptor (OR) gene superfamily. *Human Genomics*, 3(1), 87–97.
10. Jiang, Y., Gong, N. N., Hu, X. S., Ni, M. J., Pasi, R., & Matsunami, H. (2015). Molecular profiling of activated olfactory neurons identifies odorant receptors for odors in vivo. *Nature Neuroscience,* 18(10), 1446–1454.
11. Mainland, J. D., Li, Y. R., Zhou, T., Liu, W. L. L., & Matsunami, H. (2015). Human olfactory receptor responses to odorants. *Scientific Data*, 2, 150002.
12. Si, G., Kanwal, J. K., Hu, Y., Tabone, C. J., Baron, J., Berck, M., … Samuel, A. D. T. (2019). Structured Odorant Response Patterns across a Complete Olfactory Receptor *Neuron Population. Neuron*, 101(5), 950-962.e7.
13. Keller, A., Gerkin, R. C., Guan, Y., Dhurandhar, A., Szalai, B., Mainland, J. D., …

Meyer, P. (2017). Predicting Human Olfactory Perception from Chemical Features of Odor Molecules Andreas. *Science*, 355(6327), 820–826.

14. Armelin-Correa, L. M., & Malnic, B. (2018). Combining in Vivo and in Vitro Approaches to Identify Human Odorant Receptors Responsive to Food Odorants. *Journal of Agricultural and Food Chemistry*, 66(10), 2214–2218.
15. Saito, H., Chi, Q., Zhuang, H., Matsunami, H., & Mainland, J. D. (2009). Odor coding by a Mammalian receptor repertoire. *Science Signaling,* 2(60), ra9.
16. Fujita, Y., Takahashi, T., Suzuki, A., Kawashima, K., Nara, F., and Koishi, R. (2007). Deorphanization of Dresden G Protein-Coupled Receptor for an Odorant Receptor. *Journal of Receptors and Signal Transduction* 27: 323-334.
17. Sell, C. S. (2006). On the unpredictability of odor. *Angewandte Chemie - International Edition,* 45(38), 6254–6261.
18. Mainland, J. D., Keller, A., Li, Y. R., Zhou, T., Trimmer, C., Snyder, L. L., … Matsunami, H. (2014). The missense of smell: Functional variability in the human odorant receptor repertoire. *Nature Neuroscience,* 17(1), 114–120.
19. Kaupp U. B., Seifert R.; Seifert (2002). "Cyclic nucleotide-gated ion channels". *Physiol. Rev*. 82 (3): 769–824
20. Zhuang, H., & Matsunami, H. (2008). Evaluating cell-surface expression and measuring activation of mammalian odorant receptors in heterologous cells. *Nature Protocols*, 3(9), 1402–1413.
21. Bensafi, M., Rouby, C., Farget, V., Vigouroux, M., & Holley, A. (2002). Asymmetry of pleasant vs. unpleasant odor processing during affective judgment in humans. *Neuroscience Letters*, 328(3), 309–313.
22. Zhou, Y., Hallis, S. A., Vitko, T., & Suffet, I. H. M. (2016). Identification, quantification and treatment of fecal odors released into the air at two wastewater treatment plants. *Journal of Environmental Management*, 180, 257–263.
23. Van den Velde, S., Nevens, F., Van hee, P., van Steenberghe, D., & Quirynen, M. (2008). GC-MS analysis of breath odor compounds in liver patients. Journal of Chromatography B: *Analytical Technologies in the Biomedical & Life Sciences*, 875(2), 344–348.

24. Swanson, K. S., Grieshop, C. M., Flickinger, E. A., Merchen, N. R., & Fahey Jr, G. C. (2002). Effects of supplemental fructooligosaccharides and mannanoligosaccharides on colonic microbial populations, immune function and fecal odor components in the canine. *Journal of Nutrition,* 132(6), 1717-1719.
25. Saito, H., Kubota, M., Roberts, R. W., Chi, Q., & Matsunami, H. (2004). RTP family members induce functional expression of mammalian odorant receptors. *Cell*, 119(5), 679–691.
26. Von Dannecker, L.E., Mercadante, A.F. & Malnic, B. (2005). Ric-8B, an olfactory putative GTP exchange factor, amplifies signal transduction through the olfactory-specific G-protein Galphaolf. *J. Neurosci*. 25, 3793–3800
27. Kajiya, K., Inaki, K., Tanaka, M., Haga, T., Kataoka, H., and Touhara, K. (2001). Molecular bases of odor discrimination: Reconstitution of olfactory receptors that recognize overlapping sets of odorants. *Nature Neuroscience*. 3: 1248-1255.
28. Li, Y. R., & Matsunami, H. (2011). Activation state of the M3 muscarinic acetylcholine receptor modulates mammalian odorant receptor signaling. *Science Signaling*, 4(155), 1–22.
29. Ohsawa, X. I., Matsunami, X. H., & Yohda, X. M. (2019). The N-terminal region of RTP1S plays important roles in dimer formation and odorant receptor-trafficking, *J. Biol. Chem,* 294, 14661–14673.
30. Wu, L., Pan, Y., Chen, G. Q., Matsunami, H., & Zhuang, H. (2012). Receptor-transporting protein 1 short (RTP1S) mediates translocation and activation of odorant receptors by acting through multiple steps. *Journal of Biological Chemistry*, 287(26), 22287–22294.
31. Galvao, J., Davis, B., Tilley, M., Normando, E., Duchen, M. R., & Cordeiro, M. F. (2014). Unexpected low-dose toxicity of the universal solvent DMSO. *FASEB Journal*, *28*(3), 1317–1330.
32. Si, G., Kanwal, J. K., Hu, Y., Tabone, C. J., Baron, J., Berck, M., … Samuel, A. D. T. (2019). Structured Odorant Response Patterns across a Complete Olfactory Receptor Neuron Population. *Neuron*, 101(5), 950-962.e7.
33. Louis, M. (2019). Order in Odors: A Power Law Structures the Encoding of Stimulus

Identity and Intensity. *Neuron*, 101(5), 768–770.

34. Yu, Y., De March, C. A., Ni, M. J., Adipietro, K. A., Golebiowski, J., Matsunami, H., & Ma, M. (2015). Responsiveness of G protein-coupled odorant receptors is partially attributed to the activation mechanism. *Proceedings of the National Academy of Sciences of the United States of America*, 112(48), 14966–14971.
35. Reisert, J. (2010). Origin of basal activity in mammalian olfactory receptor neurons, *J. Gen. Physiol*, 136(5), 529–540.
36. Hallem, E. A., & Carlson, J. R. (2006). Coding of Odors by a Receptor Repertoire. *Cell*, *125*(1), 143–160.
37. Imai T., Suzuki M., Sakano H. (2006). Odorant Receptor-Derived cAMP Signals Direct Axonal Targeting. *Science*, 314 (5799), 657-661.
38. Verbeurgt C, Wilkin F, Tarabichi M, Gregoire F, Dumont JE, Chatelain P. Profiling of olfactory receptor gene expression in whole human olfactory mucosa. *PLoS One*. 2014;9(5):e96333.
39. Nagashima, A., & Touhara, K. (2010). Enzymatic Conversion of Odorants in Nasal Mucus Affects Olfactory Glomerular Activation Patterns and Odor Perception. *Journal of Neuroscience*, 30(48), 16391–16398.
40. Briand, L., Eloit, C., Nespoulous, C., Bézirard, V., Huet, J. C., Henry, C., … Pernollet, J. C. (2002). Evidence of an odorant-binding protein in the human olfactory mucus: Location, structural characterization, and odorant-binding properties. *Biochemistry*, 41(23), 7241–7252.
41. Robert-Hazotte, A., Faure, P., Neiers, F., Potin, C., Artur, Y., Coureaud, G., & Heydel, J. M. (2019). Nasal mucus glutathione transferase activity and impact on olfactory perception and neonatal behavior. Scientific Reports, 9(1), 1–11.
42. Trimmer, C., Keller, A., Murphy, N. R., Snyder, L. L., Willer, J. R., Nagai, M. H., … Mainland, J. D. (2019). Genetic variation across the human olfactory receptor repertoire alters odor perception. *Proceedings of the National Academy of Sciences*, 116(19), 201804106.

43. Ibarra-Soria, X., Nakahara, T. S., Lilue, J., Jiang, Y., Trimmer, C., Souza, M. A. A., … Logan, D. W. (2017). Variation in olfactory neuron repertoires is genetically controlled and environmentally modulated. *ELife*, 6, 1–29.
44. Chae, H., Kepple, D. R., Bast, W. G., Murthy, V. N., Koulakov, A. A., & Albeanu, D. F. (2019). Mosaic representations of odors in the input and output layers of the mouse olfactory bulb. *Nature Neuroscience*, 22(8), 1306–1317.
45. Nishizumi, H., & Sakano, H. (2015). Decoding and deorphanizing an olfactory map. *Nature Neuroscience*, 18(10), 1432–1433.
46. Na, M., Liu, M. T., Nguyen, M. Q., & Ryan, K. (2018). Single-Neuron Comparison of the Olfactory Receptor Response to Deuterated and Nondeuterated Odorants. *ACS Chemical Neuroscience*, 16.8b00416.
47. Li, R. C., Lin, C. C., Ren, X., Wu, J. S., Molday, L. L., Molday, R. S., & Yau, K. W. (2018). Ca 2+ -activated Cl current predominates in threshold response of mouse olfactory receptor neurons. *Proceedings of the National Academy of Sciences of the United States of America*, 115(21), 5570–5575.

요약 (국문 초록)

인간의 후각은 코에 발현된 후각 수용체에 냄새 물질이 선택적으로 결합되며 시작되며, 냄새에 의해 자극이 된 후각 수용체의 반응 조합은 냄새의 인지를 결정하는 것으로 여겨진다. 후각 수용체와 분자 사이의 결합 정도는 다양한 분자 구조적 특성과 화학적 특성에 의해 복잡한 방식으로 정의된다. 그렇기 때문에, 한 냄새 분자가 어떤 후각 수용체에 작용을 할 지, 그리고 그로 인해 어떤 냄새로 인지가 될지 예측하는 것은 매우 어려운 상황이다. 본 연구에서는, 선택된 냄새 분자에 대한 388개의 후각 수용체의 전반적인 반응 패턴에 접근하여 냄새를 분석하였다. 냄새 분자에 대한 388 개의 인간 후각 수용체의 전체 반응 패턴을 나타내는 시각화 방법이 제안되었고 수용체의 반응 패턴을 분석하고 비교하는데 사용되었다.

본 연구에서는 인돌, 메틸 디하이드로 자스모네이트 그리고 나프탈렌에 대한 인간 후각 수용체의 반응 패턴을 비교하였다. 인돌의 냄새는 농도에 따라 다르게 인지된다. 저농도의 인돌은 메틸 디하이드로 자스모네이트처럼 자스민 향을 갖지만, 고농도의 인돌 냄새는 나프탈렌과 같은 좀약 냄새와 유사하다. 인돌과 메틸 디히드로 자모네이트는 분자 구조 유사성이 낮지만, 인돌과 나프탈렌은 벤젠 고리를 포함하는 이종 고리 유사체이다. 각각의 냄새 물질에 대한 후각 수용체의 반응 정도는 Hana3A 세포에서 확립된 이종 시스템에 의해 측정되었다. 먼저, 반응하는 후각 수용체의 개수와 반응 정도는 처리된 냄새 물질의 농도와 비례함을 확인하였다. 다음으로, 388개의 후각 수용체 중, 두개 이상의 냄새 물질에 공통적으로 반응하는 후각 수용체를 구분하였다. 후각 수용체의 반응 강도는 냄새 물질의 분자 구조가 가까울 때 더 높은 유사성을 나타냈다. 관능적인 냄새의 강도와 반응하는 후각 수용체의 개수 사이에는 양의 상관 관계가 있었다. 추가적으로, 동일한 후각 수용체 아과 (subfamily) 구성원 간의 단백질 유사성을 고려하여, 후각 수용체의 아과 수준에서 후각 수용

체의 반응 패턴을 분석하였다. 두 냄새물질에 공통적으로 반응하는 아과의 개수는 공통적으로 반응하는 개별 후각 수용체의 개수보다 훨씬 많았으며, 동시에 물질 종류에 따른 패턴 특이성을 보였다. 인돌 농도가 증가함에 따라 메틸디하이드로 자스모네이트와의 유사성에 비해 나프탈렌과의 유사성이 더 증가하였다. 이는 후각 수용체의 아과 수준에서의 반응 패턴 분석이 다른 냄새들 사이의 패턴을 비교하기에 충분할 수 있음을 시사한다.

비슷한 냄새의 반응 패턴 간에 일치하는 후각 수용체 및 아과가 분석되었음에도 불구하고 각 냄새 물질에 대한 후각 수용체의 패턴들은 큰 특이성을 보였다. 이 결과는 냄새에 대한 후각 수용체의 반응이 실제로 관능적으로 인지하는 것보다 훨씬 복잡하고 구체적이라는 것을 보여준다. 이는 동물 기반 화학 물질 탐지보다 후각 수용체 기반의 기기를 이용한 화학 물질 탐지가 높은 감도와 정확성을 가질 것임을 시사한다. 또, 후각의 시각화 과정은 코 점액질과 신경계에서 발생하는 많은 자연적 메커니즘을 배제하기 때문에 제시된 냄새의 코드화 방법은 최소한의 유전자 및 개별 변이를 갖는 냄새의 객관적인 기록을 허용하고 후각의 표준화 및 냄새 감각의 추가 이해에 기여할 것이다.

주요어: 후각, 후각 수용체, 인간 후각 수용체, 냄새의 표준화, 냄새의 시각화, 냄새의 코드화, 이종 세포 발현, 인돌

학번: 2018-21289